PREPARATION AND CHARACTERIZATION OF *SHOREA ROBUSTA* BARK BASED BIOSORBENT FOR THE REMOVAL OF Cr(VI) IN DRINKING WATER

A DISSERTATION SUBMITTED FOR THE PARTIAL FULFILLMENT OF THE REQUIREMENTS FOR THE MASTER OF SCIENCE DEGREE IN CHEMISTRY

Submitted by:

POOJA REGMI

TU Exam Roll No: 1608/ /075

TU Registration No: 5-2-19-312-2014

Submitted to:

DEPARTMENT OF CHEMISTRY

AMRIT CAMPUS

INSTITUTE OF SCIENCE AND TECHNOLOGY

TRIBHUVAN UNIVERSITY

THAMEL, KATHMANDU, NEPAL

September 2022

BOARD OF EXAMINER AND CERTIFICATE OF APPROVAL

This dissertation entitled **"PREPARATION AND CHARACTERIZATION OF *SHOREA ROBUSTA* BARK BASED BIOSORBENT FOR THE REMOVAL OF Cr(VI) IN DRINKING WATER''** by Pooja Regmi, under the supervision of **Asst. Prof. Dr. Deval Prasad Bhattarai,** Department of Chemistry, Amrit Campus, Thamel, Kathmandu, Nepal is hereby submitted for the partial fulfillment of a Master of Science Degree in Chemistry. This dissertation work has been accepted for the award of a degree.

…….
Supervisor
Asst. Prof. Dr. Deval Prasad Bhattarai
Department of Chemistry
Amrit Campus, Kathmandu, Nepal

…….
Co-Supervisor
Mr. Sarad Pathak
Research Associate
Center of Research for Environment, Energy and Water (CREEW)
Kathmandu, Nepal

……
Internal Examiner
Asst. Prof. Hari Bhakta Oli
Department of Chemistry
Amrit Campus, Kathmandu, Nepal

……
External Examiner
Assoc. Prof. Dr. Surendra Kumar Gautam
Department of Chemistry
Tri-Chandra Multiple Campus,
Kathmandu, Nepal

…….
Assoc. Prof. Dr. Bhushan Shakya
Coordinator, M.Sc. Program
Department of Chemistry
Amrit Campus
Kathmandu, Nepal

…….
Assoc. Prof. Kanchan Sharma
Head of the Department
Department of Chemistry
Amrit Campus
Kathmandu, Nepal

Date: September 23, 2022

RECOMMENDATION LETTER

This is to certify that the dissertation entitled "**PREPARATION AND CHARACTERIZATION OF *SHOREA ROBUSTA* BARK BASED BIOSORBENT FOR THE REMOVAL OF Cr(VI) IN DRINKING WATER''** has been carried out by Pooja Regmi (Roll No: 1608/075, TU Regd No: 5-2-19-312-2014) as partial fulfillment of Master of Science in Chemistry under our supervision. To the best of our knowledge, this work has not been submitted to peruse any other degree in this institution.

……..

Supervisor

Asst. Prof. Dr. Deval Prasad Bhattarai

Amrit Campus

Thamel, Kathmandu, Nepal

…….

Co-Supervisor

Sarad Pathak

Research Associate

Center of Research for Environment, Energy and Water - CREEW

Baluwatar, Kathmandu, Nepal

September 13, 2022

DECLARATION

I, Pooja Regmi, hereby declare that the work presented here is genuine work done originally by me under the supervision of Assistant Professor Dr. Deval Prasad Bhattarai. This dissertation has not been published or submitted elsewhere for the requirement of a degree program. Any literature, data, or work done by others are cited in this dissertation with due acknowledgment and listed in the reference section.

……..

Pooja Regmi
Roll No: 1608/075
Department of Chemistry
Amrit Campus,
Kathmandu, Nepal
Date: September 13, 2022

ACKNOWLEDGEMENTS

First of all, I would like to express my sincere gratitude to my respected supervisor, Asst. Prof. Dr. Deval Prasad Bhattarai, Department of Chemistry, Amrit Campus, Thamel, Kathmandu, Nepal and Co-supervisor Sarad Pathak for their expert guidance, supervision, support, suggestions, and motivating me throughout this dissertation work. I extend my thankfulness to Asst. Prof. Hari Bhakta Oli for his support.

I consider it a privilege to express my gratitude to Assoc. Prof. Kanchan Sharma, Head of the Department, Assoc. Prof. Bhushan Shakya, Coordinator, Assoc. Prof. Shree Dhar Gautam, Former Head of the Department and Prof. Dr. Daman Raj Gautam, Former Coordinator of M.Sc. Chemistry and of M.Sc. Chemistry for providing me with the necessary physical facilities to carry out the research.

I am highly obliged to Mr. Bharat Dhakal and Mr. Jyoti Koirala for their help in sample collection, Dr. Ram Lal (Swagat) Shrestha for his incredible support towards the grinding the sample. I would like to thank the Nepal Academy of Science and Technology (NAST) for XRD spectra for characterizing the samples. I would like to thank the Amrit Campus department of Chemistry for FTIR spectra.

Further, I would like to express my deepest appreciation to all the teaching and administrative staff members of the Department of Chemistry, Amrit Campus for providing me the suggestions, supports, and facilities to carry out my research work. I am also grateful to my seniors and friends for their sincere co-operation, help, and encouragement during this research work. I express my gratefulness towards my senior Suresh Timalsina and companions Kuldip Joshi, Madhav Joshi, Pabita Paudel and Puja Thaneit for their help.

Finally, yet importantly, I express my deep sense of gratitude to my parents and all my family members whose constant support and encouragement lead to the successful completion of this research work.

Pooja Regmi

ABSTRACT

Activated carbons have been used in the removal of heavy metal. High surface area and porosity of activated carbon materials support in the removal of heavy metal ions. In this work, biochar has been synthesized from *Shorea robusta* bark. Excellent removal efficiency from methylene blue and iodine number can be seen in *S. robusta* treated with Zinc chloride. Due to the pHzpc of activated carbon and biochar having 6.16 and 4.62, respectively, this sorbent may effectively remove cationic Cr(VI) contaminants from alkaline aqueous solutions. Using the batch adsorption approach, the adsorption of Cr(VI) ions on biochar and chemically modified biochar of *S. robusta* has been examined in this study. The outcome demonstrates that all the factors that affected the removal of Cr(VI) by adsorption were discovered at pH 2, starting concentration of 50 ppm, equilibrium period of 120 minutes, and adsorbent dose of 50 mg. Kinetic data are presented after the pseudo second order kinetic model. By using FTIR and XRD, sample characteristics was examined. The experimental findings suggest that *S. robusta* can be used as a low-cost commercial alternative adsorbent to remove Cr(VI) from wastewater.

Keywords: *Shorea robusta, bark, biochar, activation, zinc chloride, Cr(VI)*

TABLE OF CONTENTS

LIST OF TABLES

LIST OF FIGURES

LIST OF ABBREVIATIONS

µm:	Micrometre
DW:	Distilled water
XRD:	X-ray diffraction
FTIR:	Fourier Transform infrared Spectroscopy
MB_N:	Methylene blue number
I_N:	Iodine Number
PPM:	Parts per million
RPM:	Rotation per Minute

CHAPTER 1

1. INTRODUCTION

1.1 General Introduction

Water is contaminated with various pollutants such as organic pollutants, inorganic metal ions or heavy metal ions, pathogens, etc. Due to industrial spills, accidents, discharges, and other factors, groundwater is severely contaminated with both organic and inorganic materials. Among the different possible pollutants, the increased level of trace elements such as heavy metal ions are one of the prominent causes for making water unsuitable for drinking purpose as well as for commercial applications (Patil et al., 2012). Heavy metal is a metallic element having relatively high density and the term is commonly applied to a group of metals and metalloids with atomic density greater than 4 g/cm^3. The term "Heavy metal" is intended to define some metal ions such as As^{+++}, Cd^{++}, Hg^{++}, Pb^{++}, etc. which cause detrimental effect on human health as well as ecosystem (Duruibe et al., 2007). According to World health organization (WHO) guidelines for drinking water quality, the permissible level of Chromium (VI) in drinking water are 50 ppb (0.05 mg/L or 50μg/L) (Cotruvo, 2017). The permissible limits of some heavy metals as per WHO (2017) and Nepal drinking water quality (NDWQ) standard (2008) are listed in table 1.

Table 1: *Guidelines and toxicity of most common heavy metals*

Heavy metals	WHO Guidelines (mg/L or ppm)	NDWQ standard (mg/L or ppm)
Cadmium	0.003	0.003
Mercury	0.006	0.001
Lead	0.01	0.01
Arsenic	0.01	0.05
Chromium	0.05	0.05
Zinc	0.05	3.00
Nickel	0.07	-

In the natural environment, chromium can be found in ores or in complex forms (Khalil et al., 2020). Chromium (Cr) pollution is primarily brought on by a number of industries, such as the manufacture of chromium salt, chrome mining, steel alloy

production, dye and pigment production, the textile industry, and electroplating. In nature, chromium primarily exists in two different forms: Cr(III) and Cr(VI). The precipitates $Cr(OH)_3$ and Cr_2O_3 include Cr(III), which has a negligibly low toxicity. In contrast, Cr(VI) exists as oxyanions, which are highly toxic, soluble and easy to migrate (Qin et al., 2020). As a highly oxidizing, corrosive, and carcinogenic substance, Cr(VI) is poisonous to both plants and mammals. The tenth most common element in the earth's mantle. Chromium is utilized in a variety of industrial operations, including plating, alloying and as a water corrosion inhibitor. Chromium has a wide range of oxidation states (from - 2 to + 6), however only the + 3 and + 6 states are stable in the majority of surface environment conditions. At pH ranges between 4 and 8, the first or second hydrolysis products predominate in the trivalent state, which is the most stable form under reduced circumstances. The sorption and solubility of these ions are significantly impacted by the generation of Cr(III) hydrolysis products at such a low pH (Fendorf, 1995). Only 60–80 % of the chromium that is applied during the tanning process is absorbed by the leather; the remainder is often released into the wastewaters, having a significant negative impact on the environment. In liquid tanning wastes, chromium ions are primarily found in trivalent form, which is then converted to hexavalent form (Garg et al., 2007).

A number of techniques have been developed for the removal of chromium ions from wastewater. These techniques includes ion exchanging (Rengaraj et al., 2001), precipitation and membrane process (Peng & Guo, 2020), and different electrolytic methods (Chand et al., 2014). Nevertheless, such methods are limited due to the cost factor and the production of toxin byproducts (Katheresan et al., 2018).

Adsorption method could be promising for the purification of effluent water from industries, water containing heavy metal ions, etc. As an adsorbent, various materials can be used. Activated carbon is one of the popular and easily available adsorbents and getting its preference because of its high effective surface area, high adsorption capacity, high degree of surface reactivity, and low cost of treatment process. Activated carbons from bio-waste materials have got much attention & various bio-waste materials have been tested (Moosavi et al., 2021; Reddy et al., 2016).

Many researchers have tried to prepare activated carbons from agricultural wastes, such as banana peels (Mopoung, 2008), plum kernels (Wu et al., 1999), oil palm shells (Lua et al., 2006), tea leaves (Akar et al., 2013), sawdust (Zhang et al., 2010), coffee grounds (Namane et al., 2005), coconut husk (Tan et al., 2008), jackfruit peel (Prahas et al.,

E2008) and rice husk (Cheenmatchaya & Kungwankunakorn, 2014), etc. The process of adsorption, which is surface-based, involves the diffusion of dissolved species to the porous solid adsorbent before they are stuck to its vast inner surface. The substance that is drawn to a surface is known as an adsorbate, and the material that the substance is adsorbed onto is known as an adsorbent. Adsorbent solids physically (physisorption), ionically (ion exchange), or chemically bind dissolved molecules (chemisorption) (Bonilla-Petriciolet et al., 2017).

1.2 Preparation of Activated Carbon and its Advantage

The pyrolysis of biomass produces a type of charcoal called biochar (BC), which is good for sanitizing the environment. Recent years have seen the advancement of BC's environmental applications by the successful use of this stable, porous, and extremely porous carbon material as a carrier for dispersing nanoparticles (Qin et al., 2020). Despite having a lesser adsorption capacity than activated carbon due to its weaker textural qualities, biochar is easier to produce and more ecologically beneficial. Different methods, such as microwave treatment, acid-base treatment, plasma treatment, and impregnation, have been explored to enhance the textural qualities of carbonaceous adsorbents and subsequently their adsorption capacity (Cruz et al., 2020). Chemical modifications are prioritized because they effectively enhance the biosorbent's stability and metals or metalloids, or in our instance, sorption capacity. Chemical modification can be divided into three categories: acid treatment (using sulfuric, nitric, or other acids), alkali treatment (using sodium hydroxide or potassium hydroxide, for example), and Fe salt or Fe oxide mineral coating (using minerals like ferric chloride, ferric nitrate, akaganeite, goethite, or magnetite) (Shakoor et al., 2016). Each pretreatment method is used to achieve a particular result, such as increasing chemical surface heterogeneity, increasing the quantity and dispersion of functional groups available for interaction with the metal, or changing the surface shape (Anastopoulos et al., 2018). Chemical activation normally takes place at a lower temperature than that used in physical activation. The temperature utilized for chemical activation is often lower than that for physical activation. Additionally, because chemical agents have dehydrogenation capabilities that can prevent the development of tar and lower the formation of other volatile compounds, the carbon yield in chemical activation is typically higher than in physical activation. The most often utilized

chemical activation agent is $ZnCl_2$, which produced high surface areas and high yields (Yang & Qiu, 2010).

Bark is typically treated as a waste stream in the production of timber, and because of the large volumes involved, disposal is a significant issue. The forest industry either uses bark as fuel or leaves the bark in the forest after trees are cut down.The phloem, which has an inner functional region for conduction and an outer non-functional region, the periderm, which has phelloderm, phellogen, and phellem, and the rhytidome are all parts of the structurally diverse bark. Ash-like inorganic substance is abundant in bark. Even though the mineral content may influence the ionic interaction between the metal and the bark structure and help with the ion-exchange mechanism. The ash content of barks is frequently ignored in studies on heavy metal adsorption (Şen et al., 2015). Some of the advantages od using bark-based activated carbon are listed.

- Activated carbon adsorption is frequently used to clean up groundwater so that it is safe to drink (Ferhan & Ozgur, 2011).
- Removal of contaminants like heavy metals, dye etc.
- Low cost adsorbents
- Locally available
- Excellent mechanical strength and chemical stability (Dan et al., 2021).

1.3 Selection of Biomass

In search of the new, easily available, low cost and ecofriendly adsorbent, chemically modified *Shorea robusta* bark could be a potential resource for the removal of heavy metal ions from the water source. *S. robusta* is commonly known as Saal in Nepal. From immemorial time, *S. robusta* has been used for furniture, fodder as well as biofuel. The vegetative part of the Shorea robusta is presented in the figure 1. The systemic classification of the plant is given below.

Taxonomy

Kingdom	:	Plantae
Subkingdom	:	Viridiplantae
Infrakingdom	:	Streptophyta
Superdivision	:	Embryophyta
Division	:	Tracheophyta
Subdivision	:	Spermatophytina
Class	:	Magnoliopsida
Superorder	:	Rosane
Order	:	Malvales
Family	:	Dipterocarpaceae
Genus	:	*Shorea*
Species	:	*robusta*
Common Names:		Saal tree

Figure 1:*Shorea robusta tree trunk*

The Dipterocarpaecea family includes the huge tree *S. robusta*. It is primarily found in hilly region, Tarai region especially in the Churia Range in the subtropical climate zone of Nepal. It serves as the primary supply of both raw materials for carpentry and construction projects as well as fuel wood. Waste byproducts like sawdust and wood splinters are produced as a result of the carpentry process. These byproducts actually have a high carbon content in lignocellulosic form and a unique chemical make-up, including a low percentage of inorganic components and a comparatively high percentage of volatile substances. The coal of *S. robusta* was used for brigtning the teeth before the commercial availability of toothpaste and toothbrush. The brightening action of coal could be due to high effacacy of adsorption capacity of the carbon. In this context, synthesis of activated carbon from *S. robusta* found to be imperative and it is hypothesized to develop activated carbon from the bark of *S. robusta*. Therefore, wood wastes can be employed as a precursor to create activated carbon (Shrestha et al., 2019).

1.4 Statement of Problems

Numerous methods for the removal of heavy metal ions from polluted bodies are in operation but each method has its own inherent limitation such as being expensive or creating secondary pollutants. Low cost materials with high efficacy and facile

techniques for the purification of water have yet to be developed for efficient water purification in small or large scale. Selection of appropriate method and development of effective materials for water purification is a crucial task. One of the cheaper adsorbents for the removal of heavy metal ions could be bio-sorbent which can be derived from bio-waste or biomass. The bark of *S. robusta* can be used for the preparation of biosorbent which can be eco-friendly and easily available materials.

1.5 Objectives of the Study

1.5.1 General objective

- Development of *S. robusta* bark-based activated carbon for the removal of Cr(VI) from aquesous media.

1.5.2 Specific objectives

- Synthesis of biochar from the bark of *S. robusta*
- Chemical activation of biochar by $ZnCl_2$
- Characterization of the as-synthesized biochar and activated carbon
- Determination of surface area and porosity based on the methylene blue number and iodine number method
- Study of adsorptive removal of Cr(VI) from solution using the biochar and activated carbon

CHAPTER 2

2. LITERATURE REVIEW

2.1 Development History

The earliest use of charcoal reported for the purification of drinking water dates back to 450 BC. In a Sanskrit text, filtration of water through coal after storing it in copper vessels and exposing it to sunlight has been reported. This is probably the earliest documents describing the removal of compounds from water using charcoal. But the use of activated carbon in its current form has only a short history.

Activated carbon yielded after zinc chloride treatment has high mechanical strength and high adsorptive capacities. Nowadays it has been largely superseded by the use of phosphoric acid activation (Bansal & Goyal, 2005). Activated carbon for environmental remediation and drinking water treatment has been reported in mid-20^{th} century, subsequently the wastewater treatment has been started (Purcell, 2005). Since few decades, the adsorptive removal of heavy metals from waste water and industrial effluents has been started. Industrial scale production and commercialization of activated carbon was started from early 20^{th} century (Çeçen & Aktas, 2011).

Budinova et al., (2009) studied the low cost activated carbon from bean pods waste and explored their potential application for the removal of heavy metals like As(III) and Mn(II) at different initial concentration and pH values. This process followed models of the Langmuir isotherm for both ions As(III) and Mn(II) with a capacity of 1.01 and 23.4 mg/g, respectively. The results showed that, in addition to porosity, the basic character of the carbon surfaces is an important component in the adsorption of arsenic and manganese ions.

Pandey et al., (2009) showed adsorption of Arsenic(III) to be particularly efficient in a biomass which is obtained from the plant *Momordica charantia*. This biomass was used to remove arsenic(III) under various conditions. Isotherm investigations for the As(III) ion were carried out utilizing Freundlich and Langmuir adsorption isotherms to determine the most acceptable correlation for the equilibrium curves. Both models were well-suited to the adsorption pattern. At a concentration of 0.5 mg/L of As(III) solution, the biomass of *M. charantia* was shown to be effective for the removal of As(III), with an 88 percent sorption efficiency, and therefore absorption capacity of 0.88 mg As(III)/g of biomass.

Rocha et al., (2009) carried out adsorption analysis using several types of waste rice straw as a biosorbent to adsorb Cu(II), Zn(II), Cd(II), and Hg(II) ions from aqueous solutions at room temperature. To create the ideal adsorption conditions, the effects of pH and contact time were investigated. The Freundlich equation was used to model the isotherms of adsorption. The adsorption on the rice straw was found to be in the order of Cd(II), Cu(II), Zn(II), and Hg(II). Maximum adsorptions was observed at pH 5.0, and adsorption equilibrium was reached in less than 1.5 hours. The thermodynamic characteristics of the adsorption process were examined. In order to remove the ions Cu, Zn, Cd, and Hg from actual samples of industrial effluent, the biosorbent material was utilized in columns, and its effectiveness was investigated.

Itodo et al., (2010) applied the Methylene blue and Iodine number method to estimate surface area and porosity in the activated carbon. According to estimates, the mesopore structural parameters (SMB) in 10^{-3} km^2 kg^{-1} sorbents groundnut shells (GS), sheanut shells (SS), poultry droppings (PD), and poultry waste (PW) were correspondingly 14.54–15.10, 13.54–14.01, 12.31–13.97, and 14.27–14.55. As IAN (in mlM iodine per gramme of activated carbon), their corresponding levels of activation and micropores were shown to fall in the ranges of 2.15–2.17, 2.17–2.19, 2.16–2.19, and 2.15–2.16. The findings were significantly different from those of their respective pyrolized materials and only slightly lower than those of commercial reference carbon (SMB =15.62710^{-3} km^2 kg^{-1} and IAN = 2.230 mlM/g). Efficiency of methylene blue sorption was also estimated.

Yang & Qiu, (2010) studied chemically activated walnut shells with zinc chloride to produce activated carbons. It was discovered that the ideal activated carbon had a BET surface area of 1800 m^2/g and a total pore volume of 1.176 cm^3/g when it was produced with system pressure of 30 kPa, activation temperature of 450 °C, and impregnation ratio of 2.0. SEM, TEM, and FTIR were used to characterize the prepared activated carbons. They were then utilized as an adsorbent to remove methylene blue from aqueous solutions. The results showed a positive correlation between the BET surface area and the methylene blue adsorption capability. The ideal activated carbon had a maximum methylene blue adsorption capacity of 315 mg/g. It was discovered that the Redlich-Peterson and Langmuir-Freundlich models best captured the equilibrium data, pointing to the heterogeneous surface adsorption of methylene blue on the activated carbon.

Hafshejani et al., (2015) examined the chemical and morphological structure of biosorbent through SEM, elemental analyzer, particle size analyzer, X-ray fluorescence spectroscopy, and Fourier transform infrared spectroscopy. On the biosorption of the two researched metals by nanostructured cedar leaf ash, the influence of several parameters including solution pH, contact time, and adsorbent dosage was examined. The results showed that the pseudo-second-order kinetic model could accurately describe the adsorption kinetics of Zn^{2+} and Pb^{2+} biosorption, and the Sips (Langmuir-Freundlich) model was found to fit well for Zn^{2+} and Pb^{2+} adsorption. For Pb^{2+} and Zn^{2+}, respectively, the maximum adsorption capacities were calculated as 7.23 and 4.79 mg/g.

Bonilla-Petriciolet et al., (2017) removed the heavy metals, nitrate, and phosphate ions from industrial wastewaters by using low-cost adsorbents made from dried plants. Heavy metals, nitrates, and phosphates were removed from industrial wastewaters by dried plants with the success rate of 94 percent for Cd^{2+}, 92 percent for Cu^{2+}, 99 percent for Pb^{2+}, 97 percent for Zn^{2+}, 100 percent for NO_3^-, and 77 percent for PO_4^{3-} ions.

Cruz et al., (2020) prepared biochar from corn hub and coffee husk which were carbonized in moderate circumstances and then impregnated with ZnO using a precipitation process. The resultant materials were thoroughly characterized, with textural, chemical, surface, morphological, and structural features described. The greatest results were achieved by corncob-derived ZnO impregnated biochar (CC-ZnO), which had a maximum equilibrium adsorption capacity of 25.9 mg of As (V)/g and at least 25.8 mg of Pb (II)/g.

Dan et al., (2021) evaluated the preconcentration, removal, and recovery of metal ions such as Be, Al, Co, Ni, Sr, Ag, Cd, Ba, and Pb in both batch and column mode using treated and untreated sodium hydroxide rice husk. Sodium hydroxide treatment significantly improved the removal efficiency for all metal ions of interest as compared to the untreated rice hull. The removal kinetics for Co, Ni, Zn, Sr, Cd, and Ba were extremely fast, making the treated rice husk as an attractive green adsorbent for preconcentrating, removing, and recovering low-level metal ions in column mode at high throughput. The electrostatic interaction between negatively charged rice hulls and positively charged metal ions is thought to be main mechanism for the removal of heavy metal ions. For the majority of the metal ions of interest, the performance was found best at a pH of 5. Processed rice hulls are a cost-effective alternative to the expensive resin for harmful heavy metal removal and recovery from the environment.

2.2 Chromium Removal

Franguelli et al., (2019) aims to assess the adsorption capacity of raw coconut fiber and the efficacy of Cr(VI) removal from synthetic aqueous solutions using operational parameters, carried out in a batch system, and pH 2, 270 minutes of contact time, and 10 g/L of adsorbent dosage concentration were found to be the best conditions for this metal's adsorption by the biomass. At concentrations of 25–50 mg/L, 99.2 percent removal efficiency was found for Cr(VI) solutions. When Cr(VI) solutions ranged from 100 mg/L to 250 mg/L, respectively, the removal for the highest concentrations fell from 96.3 percent to 74.4 percent. Adsorption kinetics was used and demonstrated good agreement for Elovich and pseudo-second-order models, which highlight chemisorption. The Redlich-Peterson isotherm provided the best fit for the adsorption capacity under equilibrium conditions, showing good adsorption and monolayer coverage.

Qin et al., (2020) studied ferrous sulfide nanoparticles that had been stabilized by chitosan were loaded onto biochar to generate a composite material, FeS-CS-BC, for the effective removal of hexavalent chromium from water. Batch trials were utilized to determine how well the Cr(VI) was removed. The experimental results showed that FeS-CS-BC (FeS:CS:BC = 2:2:1) eliminated Cr(VI) at a rate of 98.34%, which was significantly higher than BC (44.58%) and FeS (79.91%). In the pH range of 2–10, FeS–CS–BC effectively eliminated Cr(VI) regardless of the pH. The removal of Cr(VI) by FeS-CSBC was fitted with a hybrid chemical-adsorption reaction known as pseudo-second-order kinetics. According to the results of the X-ray photoelectron spectroscopy (XPS) investigation, Cr(VI) was decreased, and the reduced Cr(VI) was fixed on the material's surface as Cr(VI)-Fe (III)

Khalil et al., (2020) studied biochars made from rice husks and tea waste were employed to remove Cr(VI) from wastewater. With 120 mg/L starting Cr(VI) concentration at pH 5.2, TWB and RHB, in contrast, sorbed 197.5 mg/g and 195.24 mg/g Cr(VI), respectively. The best fits for the sorption of Cr(VI) onto both biochars were found in the pseudo-second order model and Langmuir (monolayer sorption) models, according to kinetic and isotherm modeling data. According to FTIR, the functional groups -OH, -COO-, and -NH_2 were implicated in the sorption of Cr(VI) onto biochars. Both types of biomass were used to make biochar, which efficiently removed Cr(VI) from contaminated water. However, TWB's sorption capacity was

somewhat higher than RHB's. Some of the literatures for the removal of Cr(VI) from wastewater are listed in table 2.

Table 2: *Activated carbon prepared from different biomass and their removal efficacy*

S. N.	**Raw material**	**Ions**	**pH**	**Contact time**	**Adsorption capacity**	**Kinetics**	**Ref.**
1.	South African coal	Cr(VI)	below 3	-	3 mg/g	Langmuir isotherm, Pseudo-first order kinetics	Di Natale et al., 2007
2.	Olive stones	Cr(VI)	Suitable pH: 1.5	90 minute	71 mg/g,	Langmuir adsorption isotherm, Pseudo first order kinetics	Attia et al., 2010
3.	Corn cob	Cr(VI)	4.0	-	11.1 mg/g,	Pseudo-second order kinetics	Kumari et al., 2018
4.	Cornus mas, *Rosa canina*, *Musa cavendishii* peel	Cr(VI)	Effective pH: 2-3,	Eq. time: 60 min	10.42, 15.17 and 6.81 mg/g, respectively	Langmuir adsorption model and pseudo-second order kinetics	Parlayici & Pehlivan, 2019
5.	Spent coffee	Cr(VI)	Suitable pH: 3	-	109 mg/g,	Langmuir	Asimakopoulos et al., 2020
6.	*Manihot esculenta*	Cr(VI) and Co(II)	Natural solution pH	180 minute	166.35 mg/g for Cr(VI) and 301.63 mg/g for Co(II)	Langmuir model, Pseudo-second order	Belcaid et al., 2021

Number of AC from different biowastes with promising efficiencies have been reported however the surface area of the activated carbon, abundance of biowaste, and porosity are still to be considered. The porosity and surface area of the activated carbon depends on the orientation of lignocellulosic materials in the biowaste and that differs among the biowastes.

CHAPTER 3

3. MATERIALS AND METHODS

3.1 Instruments and Chemicals used

Instruments like Grinder, Sieve no. 250µm, Weighing balance (Phoenix, PH2204C), Hot air oven, Muffle Furnace, Auto Deluxe Digital pH meter (Labrotonics-11, India), Rotatory Flask Shaker, Filter Paper (Whatman-1, 125µm), Double Beam UV Visible Double Spectroscopy (Labrotonics-2802), FTIR (PerkinElmer 10.6.2) and the chemicals like methylene blue (Mol. mass = 373.90, 98.5 % purity, Nacalai tesque), Hydrochloric acid (36 %, Qualigens), Sodium thiosulphate (molecular mass=248.18, 99 %, Qualigens), Potassium dichromate (molecular mass=294.18, Fischer scientific), Iodine (253.8 molecular mass, Sara Bhai), Potassium iodide (Qualigens), Diphenyl carbazide (248.28 g/mol, Loba chemie) were used. Chemicals used were all of laboratory grade and were used as received without any further purification.

3.2 Sample collection

Bark of *Shorea robusta* was collected from the Nareshwar, Gorkha district (Latitude: 28.02, Longitude: 84.61) and washed with tap water followed by chopped into small pieces with knife. These small pieces were washed with tap water and then by distilled water (conductivity of distilled water: 8.5 µSiemen/cm). The washed and chopped bark was dried over sunlight for a week. Then the sample was dried in a hot air oven (at 80 °C for 8 h) in muffle furnace and grinded with an electric disintegrator to obtain fine powder. The powder was sieved through 250 µm seized sieving mesh to obtained fine powder.

Figure 3.1: *Google map of the sample collection area*

3.3 Preparation of Adsorbents

3.3.1 Preparation of biochar

235.4 g of fine powder of *S. robusta* was charred by conc. sulphuric acid which was added slowly and stirred by glass rod until brown color of powder turns into black and left for 24 h at room temperature. This is biochar. The biochar was washed with distilled water until it become neutral. At neutral condition, it was dried into oven at 100 ± 10 °C and grinded the biochar with mortar and pestle to produce fine powder.

3.3.2 Preparation of activated carbon

A series of zinc chloride activated carbon was generated in order to determine the optimum conditions for the synthesis of pretreated biochar from the powdered precursor. For this, powdered precursor was activated with 50 % zinc chloride solution at various ratios and temperatures in a muffle furnace. The activated carbon was cooled to room temperature and washed with distilled water until the pH was neutral. Finally, it was dried in a hot air oven at 110 °C and stored in an airtight vial tubes for further research.

3.4 Reagent preparation

3.4.1 1000 ppm methylene blue stock solution

0.2922 g of hydrated methylene blue was dissolved in distilled water in a 250 mL-volumetric flask and diluted up to the mark. Then the stock solution was diluted to 100 ppm and to 10 ppm. Finally, 1 to 9 ppm of methylene blue solutions was prepared by serial dilution method.

3.4.2 Preparation of 5 % HCl

69.44 mL of 36 % HCl was added into about 400 mL of distilled water in 500 mL volumetric flask in installment wise in a fume cupboard with frequent shaking the solution. Finally, the solution was made up to the mark.

3.4.3 Preparation of 0.1 N Sodium thiosulphate solution

12.41 g of sodium thiosulphate was dissolved in approximately 75 mL of freshly boiled and cooled distilled water. 0.05g of sodium carbonate was added to minimize bacterial decomposition of the thiosulphate solution and transferred the mixture in 500 mL volumetric flask and diluted up to the mark.

3.4.4 Preparation of 100 mL of 0.1 N $K_2Cr_2O_7$ solution

0.4903 g of potassium dichromate was dissolved in 100 mL volumetric flask and diluted up to the mark with distilled water.

3.4.5 Preparation of 0.1 N iodine solution

6.35 g of iodine crystal and 9.55 g of potassium iodide was mixed in a beaker. 5 mL of distilled water was added into the beaker and stirred well. Further added 5 mL DW each time with constant stirring and made the volume to about 50 mL. The solution was allowed to stand for a minimum period of 4 hours to ensure complete dissolution of iodine crystal. The solution was transferred in volumetric flask of 500 mL capacity and distilled water was added up to the mark. Flask was shaken well to make the solution homogeneous. The solution was rightly enclosed in dark to ensure to cut off the light radiation.

3.4.6 Preparation of 10 % starch solution

10 g of starch solution was added into 100 mL of water and boiled for 15 minutes.

3.4.7 Standardization of sodium thiosulphate

Burette was rinsed with distilled water followed by as-prepared sodium thiosulphate solution (approx. 0.1 N) and filled with it up to the zero mark. 10 mL of standard $K_2Cr_2O_7$ solution was pipetted in to a conical flask containing half test tube distilled water. 2 mL of Conc. HCl and one test tube 5 % KI solution was added into the conical flask. Mixture was covered with a watch glass, shaken well and was kept in dark for about 5 minutes. The watch glass and inner wall of conical flask was rinsed with 10 mL of distilled water so as to trap vaporized I_2 in the solution. The solution was titrated with sodium thiosulphate solution with constant shaking until faint yellow colour appeared. About 2 mL of starch solution was added when the color of the titrant was like a straw color. Upon addition of starch, the color of solution was changed to dark blue color. This is due to absorption of iodine by starch solution. More sodium thiosulphate was added drop by drop until blue color got discharged. The volume of thiosulphate consumed was noted and its concentration was calculated. After calculation, the concentration of sodium thiosulphate was determined to be 0.094 N.

3.4.8 Standardization of iodine solution

25.0 mL of iodine solution was pipetted into the 250 mL conical flask and was titrated with standardized sodium thiosulphate solution until the iodine solution was light yellow color. Few drops of starch indicator was added and titrated continue drop wise until one drop produces a colorless solution. The volume of thiosulphate solution from burette was noted and the concentration of iodine was calculated. After calculation, the concentration of iodine was determined to be 0.089 N

3.4.9 Preparation of exactly 0.05 N sodium thiosulphate solution

132.9 mL of 0.094 N sodium thiosulphate solution was taken in 250 mL volumetric flask and the distilled water was added up to mark.

3.4.10 Preparation of Cr(VI) solution

3.73 g of potassium chromate (K_2CrO_4) was added in 1000 mL of volumetric flask and distilled water was added up to the mark.

3.4.11 Hydrochloric acid solutions (1M)

8.6 mL of 35 % concentrated hydrochloric acid was added to 50 mL of distilled water and distilled water was added slowly up to the mark level.

3.4.12 Sodium hydroxide (1 M)

4 g of sodium hydroxide was transferred into 100 mL volumetric flask and distilled water was added up to the mark. The concentration was ensured.

3.4.13 Coloring reagents (DPC)

0.0625 g of Diphenylcarbazide was dissolved in 12.5 mL acetone in 25 mL volumetric flask and distilled water was added up to the mark.

3.5 Characterization of Adsorbents

As-prepared biochar was characterized by methylene blue number and iodine number to determine the surface area and mesoporosity. The functionality of the activated carbon was determined by FTIR spectroscopy method and crystallinity was determined by XRD analysis.

3.5.1 Determination of methylene blue number

The methylene blue adsorption method of activated carbon was determined by batch adsorption experiments. 0.05 g of activated carbon was mixed with each 100 mL of different concentration i.e. 25, 50, 100, 150, 250 and 300 ppm of methylene blue solution and was agitated for four and half hour in a shaker at 225 rpm and left for about 24 hour. Solution was filtered using Whatmann (42) filter paper and filtrate of solution was analyzed for residual concentration by using a spectrophotometer.

The amount of methylene blue adsorbed (q_t) uptake per unit mass of the adsorbent (mm/g) at time t is given by the equation.

$$q_t = \frac{(C_0 - C_e) \times \mathrm{V}}{w} \quad \ldots (1)$$

Here C_0 and C_e are initial and equilibrium final concentration of methylene blue solution in mg/L (ppm), respectively. W is the weight of the adsorbent taken in gram and V is the volume of solution taken in litre.

3.5.2 Determination of iodine number

0.1 g of AC was added to each 5 mL of 5% hydrochloric acid (HCl) in three conical flasks (for triplicate reading) and swirled until all the AC was thoroughly wetted by acid. The solution was boiled and cooled down to room temperature. To this, 10 mL of 0.1 N iodine solution was added. The solution was shaken thoroughly for 15 minutes using a shaker (200 RPM). Then the solution was allowed to settle and was filtrate using filter paper. The filtrate was titrated against 0.05 N sodium thiosulphate solution. Just after the appearance of straw yellow color few drops of freshly prepared starch (indicator) were added as indicator. The solution become dark blue which was titrated against sodium thiosulphate until it becomes colorless. The difference in concentration of iodine was adsorbed by AC. Then the iodine number was determined by using formula

$$\text{Iodine number } \left(\frac{\text{mg}}{\text{g}}\right) = \frac{Amount\ of\ iodine\ in\ (milligram) adsorbed\ by\ carbon}{weight\ of\ carbon\ taken\ in\ gram} \quad \ldots (2)$$

3.5.3 Point of zero charge

0.1 g of AC was added to 50 mL of 0.1 M $NaNO_3$ solution at room temperature at nine flasks. The pH values of 2, 3, 4, 5, 6, 7, 8, 9, and 10 were maintained using 0.1 M HCl and 0.1 M NaOH, where necessary. After vigorous shaking for 48 hours, the solution was allowed to settle down. The content was filtered and pH of each solution was

measured. The difference in pH was calculated for each solution. For the adsorbent, pH_{PZC} is the initial pH value at which pH = 0. From the graph, it illustrates the link between starting pH and equilibrium pH.

3.5.4 X-ray Diffraction (XRD) Spectroscopy

The diffraction analysis was performed on AC sample to determine the degree of crystalline or amorphous nature of the AC. The crystallinity or amorphous of the saal based AC samples was studied using Rigaku Multiflex diffractometer with monochromatic CuKα radiation of wavelength 1.5406 Å. XRD scanning was performed under ambient conditions over the 2θ region of 10°-80° at a rate of 2°/min (40 kV, 20 mA) in Nepal Academy of Science and Technology (NAST) Khumaltar, Lalitpur, Nepal.

3.5.5 Fourier Transform Infrared (FTIR) Spectroscopy

FTIR spectrometric measurement of the biochar and activated carbon was done at the Department of Chemistry, Amrit Campus, and Kathmandu, Nepal. Spectra of the samples were documented using Perkin Elmer Spectrometer 10.6.2 version. The background correction was accomplished by using isopropanol. All the spectral data were collected from 450-4000 cm^{-1} cutoff range with 4 cm^{-1} resolution.

3.5.6 Determination of λ_{max} and calibration curve for methylene blue

Methylene blue was diluted from a 1000 ppm stock solution to 100 ppm, which was then further diluted to 10 ppm to determine the maximum concentration. Then, from the 10 ppm solution, 1-10 ppm solution was made. A solution with a 10 ppm concentration was taken in a glass cuvette with a 1 cm path length, and the absorbance was calculated using a wavelength range of 300 to 800 nm. Further graphing of the absorbance at each wavelength was done. Maximum wavelength (λ_{max}) refers to the absorbance that is greatest at a particular wavelength. Methylene blue solutions of concentration 1–10 ppm were used for setting calibration curve. The absorbance of each solution was determined at its 660 nm maximum wavelength. The concentration vs. absorbance graph was drawn. The graph of absorbance vs. concentration is referred to as the calibration curve.

3.6 Adsorption Study

The adsorption parameter such as pH of the solution, initial concentration of Cr(VI), contact time of the adsorption process were investigated. The working solution of various required concentration was prepared by diluting the stock solution. Filter paper (Whatman no. 1) was used to filter the contents of these flasks, and the filtrate's concentration was measured. The absorbance of Cr(VI) was measured using the 1,5-Diphenylcarbazide spectrophotometric technique.

According to the following calculations, specific metal uptake:

Adsorption capacity (q_e) = $\frac{(C_0 - C_e) \times V}{w}$ … (3)

Where Ci and Ce stand for the initial and equilibrium concentrations of metal ions, respectively. V stands for the volume (L) of the metal solution and w for the gram weight of the biomass.

Metal ion removal percentage calculation: The percentage of complexed metal in relation to the initial concentration of metal ions was expressed as follows:

$$Removal\ \% = \left(\frac{C_i - C_e}{C_i}\right) \times 100 \quad \ldots (4)$$

Whereas Ci and Ce represent the initial and final concentrations of respectively, metal ions (Verma et al., 2017).

3.6.1 Effect of pH

In this experiment, pH studies were performed by shaking 25 mL of 25 ppm of Cr (VI) solution containing 25 mg of carbon sample (biochar and ctivated carbon) in a bottle. The pH solution was adjusted from 1-8 using 0.1 N HCl and 0.1 N NaOH solution, where necessary. Each bottles was then agitated in a shaker maintained at room temperature and 200 rpm for about 5 hours to attain the equilibrium. The filtrate was used for determination of Cr(VI) concentration.

Initial concentration was studied by shaking each bottle containing 50 mL of 25 ppm, 50 ppm, 100 ppm, 150 ppm, and 200 ppm Cr(VI) solution at optimum pH with 50 mg of activated carbon. The reagent bottles were subsequently placed on a shaker for 5hrs at an agitation speed of 200 rpm at room temperature. After this, the solution was filtered and the absorbance of solution was measured for the determination of the final concentration. Cr (VI) concentration before and after adsorption were determined spectrophotometrically.

3.6.2 Effect of dosages

In this experiment, the effect of dosages was studied by shaking each 50 mL of Cr(VI) solution provided with 10 mg, 20 mg, 40 mg, 50 mg, 60 mg, 80 mg and 100 mg of carbon in different reagent bottle at optimum pH and optimum concentration condition. The reagent bottles were subsequently placed on a shaker for 5 hrs at an agitation speed of 200 rpm at room temperature. After this, the solution was filtered and the absorbance of solution was measured for the determination of the final concentration. Cr (VI) concentration before and after adsorption were determined by using UV-visible spectrometer. By using this data, adsorption Isotherm of Cr (VI) can be determined.

3.6.3 Adsorption kinetics

In a series of batch mode studies, the adsorption kinetics of Cr(VI) were investigated. In these experiments, different reagent bottles containing 50 mL of 50 ppm Cr(VI) solutions with an adsorbent dye of 50 mg activated carbon and biochar were shaken at 200 rpm for 30, 45, 60, 75, 90, 120, 150, and 180 minutes at room temperature. After the desired contact time, the sample was removed and filtered. Finally, a UV-visible spectrometer was used to analyze the absorbance of the filtrate solution.

CHAPTER 4

4. RESULT AND DISCUSSION

4.1 Preparation of biochar and activated carbon

The powder form of *S. robusta* bark upon treatment with concentrated sulphuric acid produces a black mass which is termed as biochar. As a general rule, concentrated sulphuric acid has strong dehydrating action upon carbohydrates or its derivative causing its dehydration and producing carbon. The process is often termed as charring. Charring is carried out by heating (burning or pyrolysis) or some sorts of chemical treatment (e.g., treatment with sulphuric acid). The char obtained from biomass is termed as biochar. Since, biomass consist of volatile materials, a porous structure is formed upon pyrolysis. The surface structure, internal structure and composition varies with the nature of biomass, method of charring and processing. That is why, the biocharr obtained from different biomass varies considerably. As a rough estimate, hemicellulose mass gets decomposed at 220 °C, cellulose mass gets decomposed at 280 °C and lignin gets decomposed at 200–500 °C.

In general,

$$\underset{\text{Carbohydrates}}{C_n(H_2O)n} + \underset{\text{Sulphuric acid}}{\text{conc. } H_2SO_4} \longrightarrow \underset{\text{Char}}{n\,C} + \underset{\text{hydrated sulphuric acid}}{H_2SO_4.n\,H_2O}$$

Based on this principle, the charring of cellulose or carbon materials can be displayed in terms of reaction as,

$$\text{Sample (lignin + cellulose + hemicellulose)} + H_2SO_4 \rightarrow \text{Carbon} + H_2SO_4\,xH_2O$$

The biochar is carbon rich material with profound surface area and porosity. During the process of charring, some tar product may clog the carbonaceous pore. Therefore, activation of biocharr was carried out in this work. The biochar was pre-carbonized at temperatures (280-300 ℃) in the muffle furnace. At that temperature, some volatile compounds were supposed to be removed with the development of porosity. At that carbonization temperature, volatile compounds were also assumed to be lost. Activation made the raw carbon material porous. In this research work, phosphoric acid was used as activating agent. All in all, the yield and reactivity of char is a function of biomass source, pyrolysis condition such as temperature, heating rate, particle size and residence time. As prepared biochar and activated carbon were used for further processing of characterization and its application for the removal of heavy metal ions of chromium.

4.2 XRD analysis

Figure 4.1 shows the XRD of activated carbon at 200 °C and 300 °C. This graph shows that all carbon materials were found amorphous with a surface that was slightly microcrystalline. Since there are no other peaks, all the carbons must exclusively include carbonaceous elements and no other contaminants.

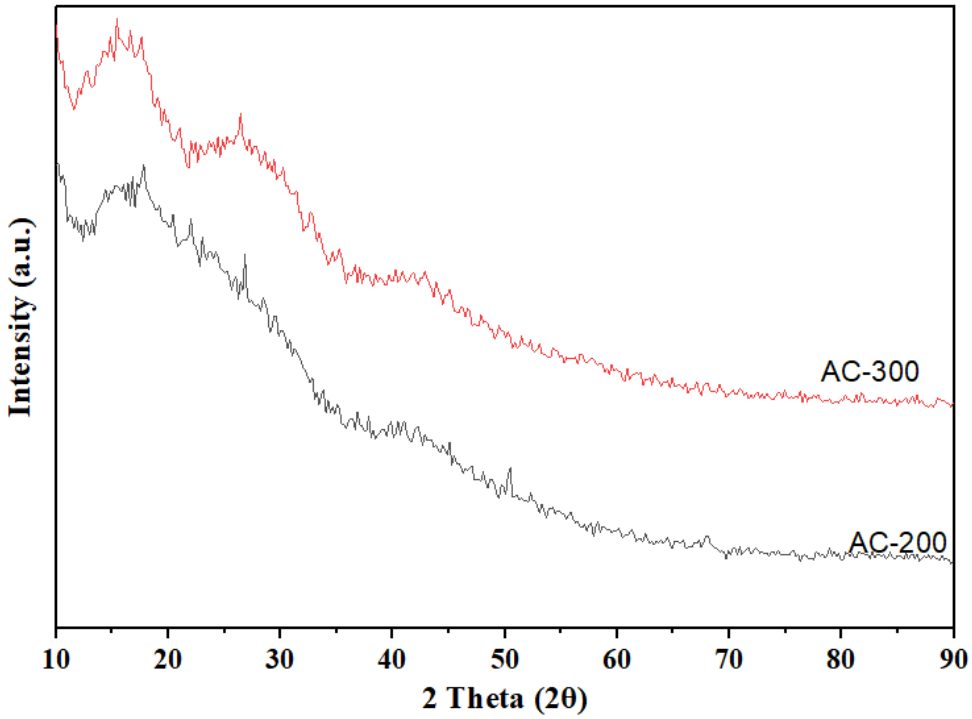

Figure 4.1: *XRD spectra of activated carbon at 300 °C and 200 °C temperature.*

4.3 Fourier Transformed Infra-Red Spectra

For the purpose of interpreting infrared spectra, it is important to correlate the absorption bands in the spectrum of an unknown molecule with the known absorption frequencies for the various kinds of bonds (Figure 4.2). The strength (weak, medium, or strong), form (wide or pointed), and position (cm^{-1}) of an absorption band in the spectrum can all be used to identify the cause of the phenomenon (Pandey et al., 2009). The broad peak in the range of 3200-3600 cm^{-1} (approximately at 3400 cm^{-1}) is assigned to stretching vibration of O-H bonds of alcohol or phenol or adsorbed moisture. The peak around 1600 cm^{-1} is may be attributed to C=C stretching vibration in the aromatic ring. The band at 1680–1770 cm^{-1} represents the acidic carbonyl C=O stretching and peak at 1715 cm^{-1} is attributed to the vibration of – COOH band.

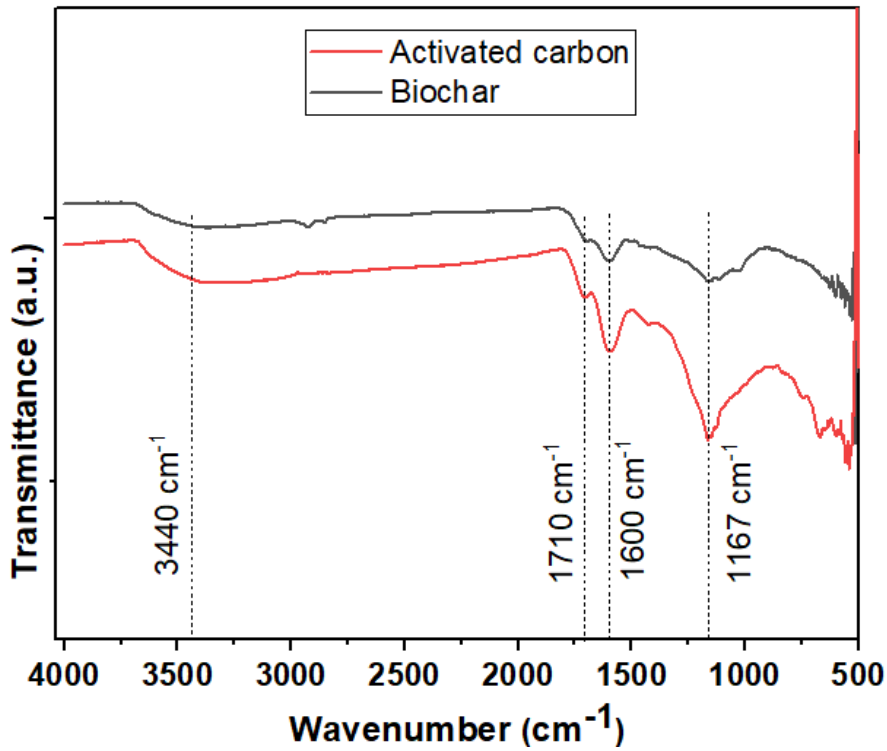

***Figure 4.2**: FTIR spectra of biochar and activated carbon*

4.4 Porosity Determination of Adsorbent

4.4.1 Iodine number

Iodine number of the biochar and activated carbon were studied. Before proceeding iodine number experiment, the standardization of sodium thiosulphate and the iodine solution were carried out. Then these solutions were diluted as per requirement.

The iodine number gives the information about the micropores present in the activated carbon. To carry out iodine number experiment, to the 5 mL of 5 % HCl and 0.1 g of activated carbon 10 mL of 0.89 N iodine solution was added. The solution was shaken thoroughly for 15 minute using a shaker (250 rpm). Then the solution was allowed to settle and was filtered using filter paper. The filtrate was titrated against 0.05N sodium thiosulphate solution. Iodine number of the biochar and activated carbon (activated in different ratio and at different temperature) was calculated using following equations.

Calculation of iodine consumed by 0.1 g of AC

I_2 consumed = No. of milligram of I_2 consumed – No. of milligram of I_2 consumed

= Vol. of I_2 solution × conc. of I_2 before adsorption – Vol. of I_2 solution × conc. of I_2 after adsorption

… (5)

$$\text{Iodine number} = \frac{Amount\ of\ iodine\ in\ (miligram) adsorbed\ by\ carbon}{weight\ of\ carbon\ taken\ in\ gram}\ \text{mg/g} \quad \ldots (6)$$

The calculation shows the following value of iodine number for the as-prepared activated carbon.

Table 4.1: *Table- showing iodine number of biochar and activated carbon.*

SN	Samples	Iodine number (mg/g)
1	Biochar	125.73
2	$ZnCl_2$ treated Carbon (1:3)	1520.00
3	$ZnCl_2$ treated Carbon (1:4)	1435.10
4	$ZnCl_2$ treated Carbon (1:5)	1676.40
5	Pretreated $ZnCl_2$ Carbon (1:5) 200 ℃	1145.54
6	Pretreated $ZnCl_2$ Carbon (1:5) 300 ℃	1272.54
7	Pretreated $ZnCl_2$ Carbon (1:5) 400 ℃	929.64

Iodine number is the amount of iodine in milligram adsorbed bye one gram of carbon. As the size of iodine is small its size is similar to that of micropore range. Therefore, iodine number indicates the concentration of micropore in the AC. Iodine number of *S. robusta* bark based biochar and activated carbon are plotted in figure 4.3. It is the most basic criterion to measure the efficiency of activated carbon. Higher values of iodine number suggests more porosity and higher levels of activity (Itodo et al., 2010). The iodine number of biochar and activated carbon are 125.73, and 1272.54 mg/g, respectively.

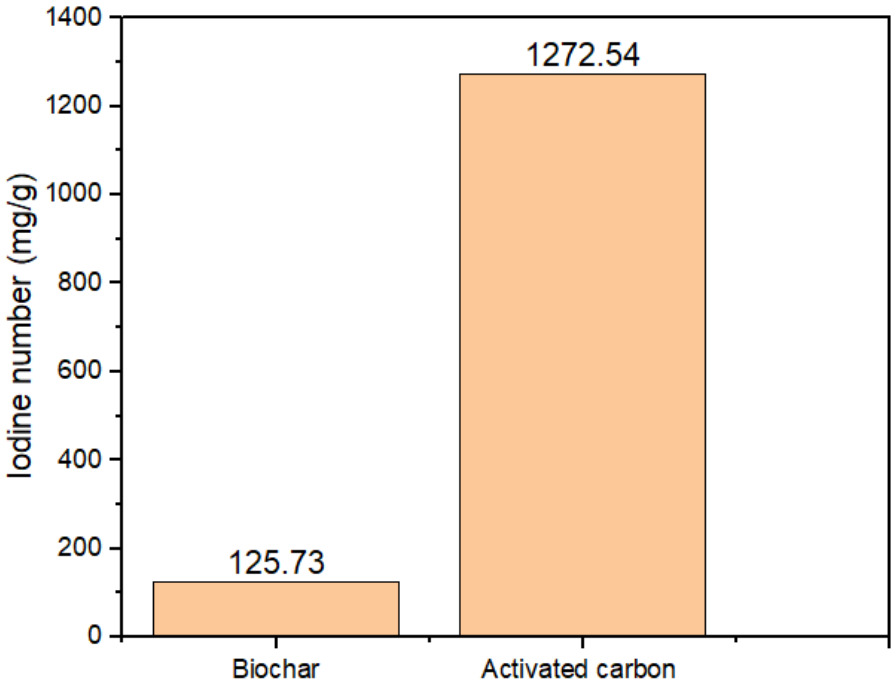

Figure 4.3: *Bar diagram showing average iodine number of biochar and activated carbon. The iodine number values are expressed in mg/g unit.*

4.4.2 Methylene blue Number

Methylene blue number of the biochar and activated carbon was measured by recording the absorbance in UV spectrophotometer in the wavelength window of 300-800 nm. The maximum absorbance of MB from a plot of absorbance with concentration in ppm λ_{max} is 660 nm is shown in graph below (Figure 4.4). The goal of instrument calibration is to remove or significantly minimize bias in an instrument reading throughout a range for all continuous values. In order to optimized its performance, a UV visible spectrophotometer's calibration was performed (Adeeyinwo et al., 2013). The absorbance of 1 to 9 ppm concentration of methylene blue solution was measured by UV visible spectrophotometer and finally plotted curve of absorbance versus concentration. It was determined from the graph that the linear model provides the least R-squared (0.9994), which is the minimum when compared to the sum of the residual range, thereby confirming the accuracy of the results and the functionality of the instrument. The curve fitting for the normal calibration gave the results using calibration model with least square value chosen as performance measure (R^2).

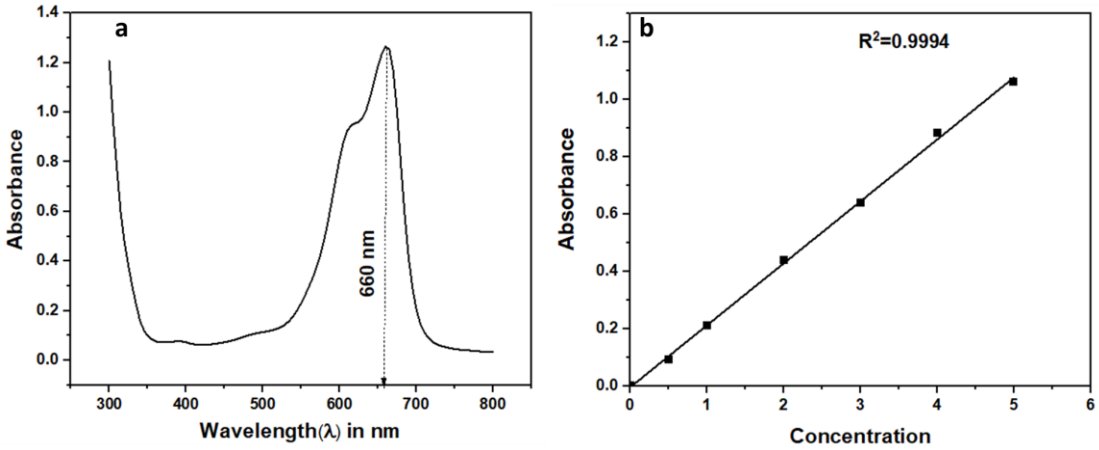

Figure 4.4 ***(a):*** *Maximum wavelength of methylene blue in aqueous solution and (b) Calibration curve for the determination of MB number*

Methylene blue number of *S. robusta* bark based biochar and activated carbon are displayed in table 4.

Table 3.2: *Table showing methylene blue number of the biochar and activated carbon*

Sample	Ratio	Initial conc. (ppm)	MB_N (mg/g)
Biochar		100	124.14
Activated Carbon	(1:3)	100	131.14
Activated Carbon	(1:4)	100	131.06
Activated Carbon	(1:5)	100	159.8
Activated Carbon	200 ℃	100	130.22
Activated Carbon	300 ℃	100	147.60
Activated Carbon	400 ℃	100	139.56

The average methylene blue number of biochar and activated carbon is 124.14 and 147.60 mg/g, respectively at 100 mg/L as shown in figure 4.5.

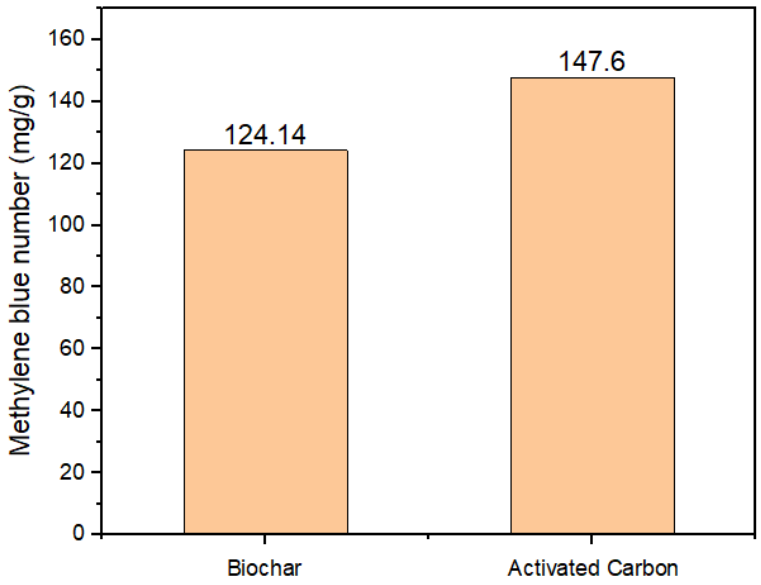

Figure 4.5*: Average methylene blue number of the biochar and activated carbon. The methylene blue number values are expressed in mg/g unit.*

4.5 Point of Zero Charge (PZC)

Point of zero charge is the pH level at which an adsorbent (such as activated carbon) has no net charge. A plot of change in pH versus initial pH is plotted (Figure 4.6). Due to the presence of functional groups like OH-, COO-, etc. above the pH_{PZC}, the adsorbent is negatively charged. At pH levels greater than pH_{PZC}, cationic ion adsorption is preferred. Under the pH_{PZC}, the adsorbent has a positive charge. Anionic dye adsorption is advantageous at pH_{PZC}.

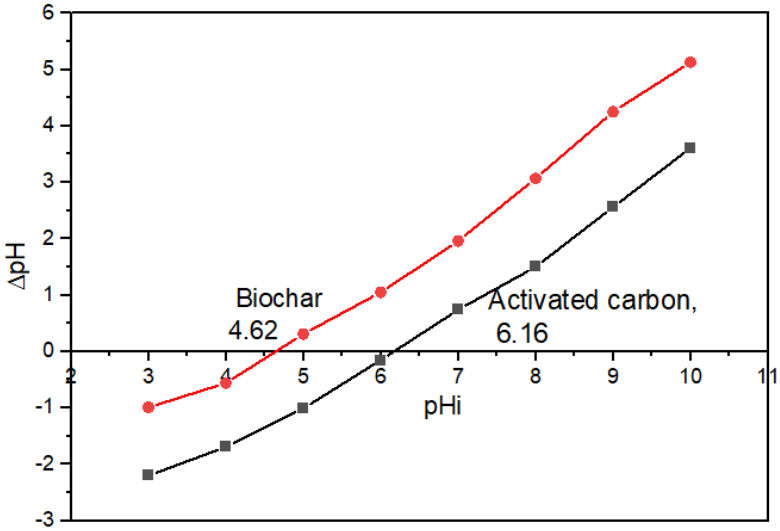

Figure 4.6: *Diagram showing PZC value of biochar and activated carbon*

4.6 Calibration curve of Cr (VI)

For the optimization of absorbance dose, concentration effect, pH effect, agitation time effect, spectroscopic tool was used. Maximum absorbance of Cr(VI) solution was measured at 370 nm. For determination of λmax and calibration curve, the absorbance of 1 to 20 ppm Cr(VI) solutions were used. A curve of absorbance versus wavelength (Figure 4.7 (a)) and absorbance versus concentration of the solutions (Figure 4.7 (b) were plotted in order to find λmax and calibration curve, respectively. It was determined from the graph that the linear model provides the least R-squared (0.994), which is the minimum when compared to the sum of the residual range, thereby confirming the accuracy of the results and the functionality of the instrument. The curve fitting for the normal calibration gave the results using calibration model with least square value chosen as performance measure (R^2).

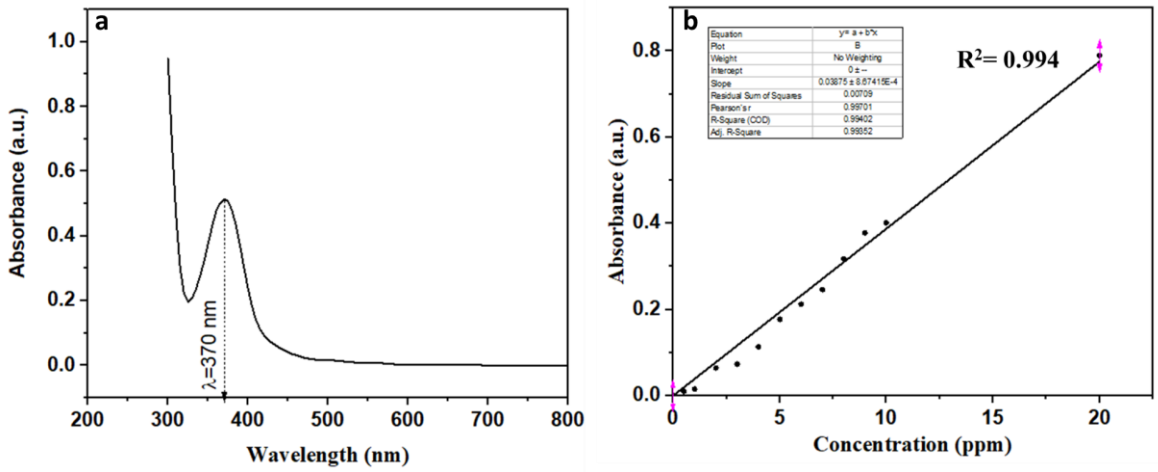

Figure 4.7: *(a) Maximum wavelength for determination of Cr(VI) (b) Calibration curve for determination of Cr(VI)*

4.7 pH Effect

The type and ionic state of the functional groups on the adsorbent and the metal chemistry in solution can both have a significant impact on how sensitively metal adsorption is affected by pH. Chromium ions co-exist in a range of pH values from 1.0 to 6.0 in the forms of $Cr_2O_7^{2-}$, $HCrO_4^-$, $Cr_3O_{10}^{2-}$, and $Cr_4O_{13}^{2-}$, with $HCrO_4^-$ predominating. The dominating species are CrO_4^{2-} and $Cr_2O_7^{2-}$ as the pH of the solution rises. More adsorption at an acidic pH suggests that the lower pH causes an increase in H^+ ions on the adsorbent surface, which leads to a noticeably strong electrostatic

attraction between positively charged adsorbent surface and chromate ions. The dual competition between the anions (CrO_4^{2-} and OH^-) to be adsorbed on the surface of the adsorbent, of which OH^- predominates, may account for the reduced adsorption of Cr(VI) at pH levels greater than 6.0. Additionally, it has been proposed that in the presence of an adsorbent, Cr(VI) could be converted to Cr(III) under acidic circumstances. The increased adsorption in the acidic zone is likely to be caused by the oxidation of the CrO_4^{2-} and $Cr_2O_7^{2-}$ ion to Cr^{3+}. Positively charged species can easily take its place due to its small size (Noor et al., 2017). Additionally, for pH values below 6.16 and 4.62, positively charged (pHzpc) particle surfaces of activated carbon (zinc chloride treated) and untreated biochar are adsorbed by Cr(VI) by electrostatic attraction and/or by the binding of $HCrO_4^-$ to surface acidic functional groups (Moussavi & Barikbin, 2010). The maximum percentage removal of Cr(VI) was observed at pH 2 (Figure 4.8).

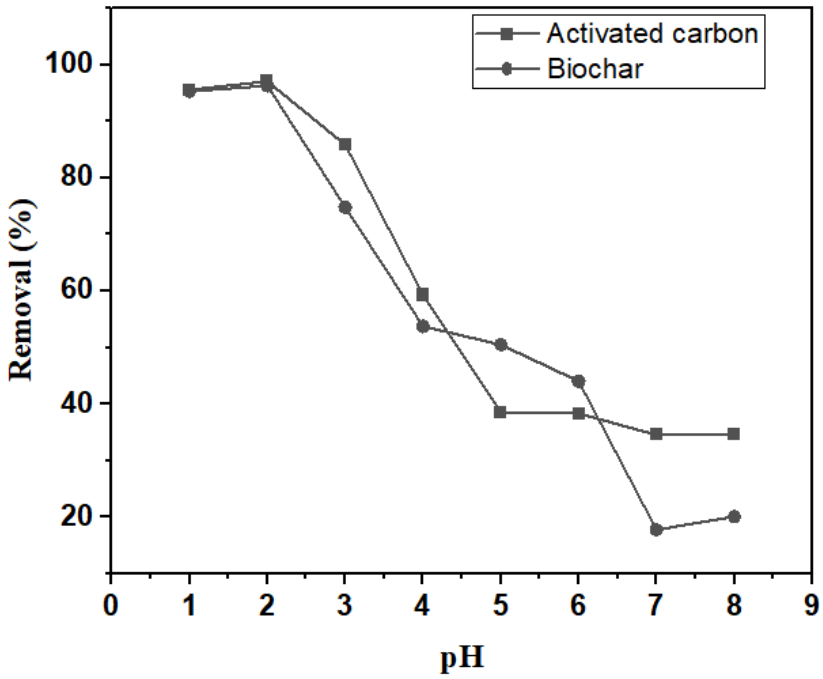

Figure 4.8*: pH effect for the removal of Cr(VI)*

4.8 Effect of Concentration

The amount of Cr(VI) that is present after treatment compared to before treatment depends on the initial concentration. With the adsorbent dosage and contact duration stayed constant at 50 mg and 5 hours, respectively, Cr(VI) solution was kept at its optimum pH 2 level. The proportion of Cr removal is significantly influenced by the initial Cr content. The quantity of Cr uptake (qe) and % elimination are plotted against

the initial concentration of Cr(VI) solution in Figure 10. According to experimental findings, Cr(VI) adsorption gradually increased up to a starting value of 25 ppm. Adsorption is increased gradually until it reaches a starting concentration of 50 ppm (Figure 4.9). The initial concentration is unaffected by adsorption once Cr(VI) has attained its maximum absorption (qe). The immediate relationship between the concentration of the Cr(VI) and the binding sites on an adsorbent surface determines how the initial Cr(VI) concentration factor will affect the process.

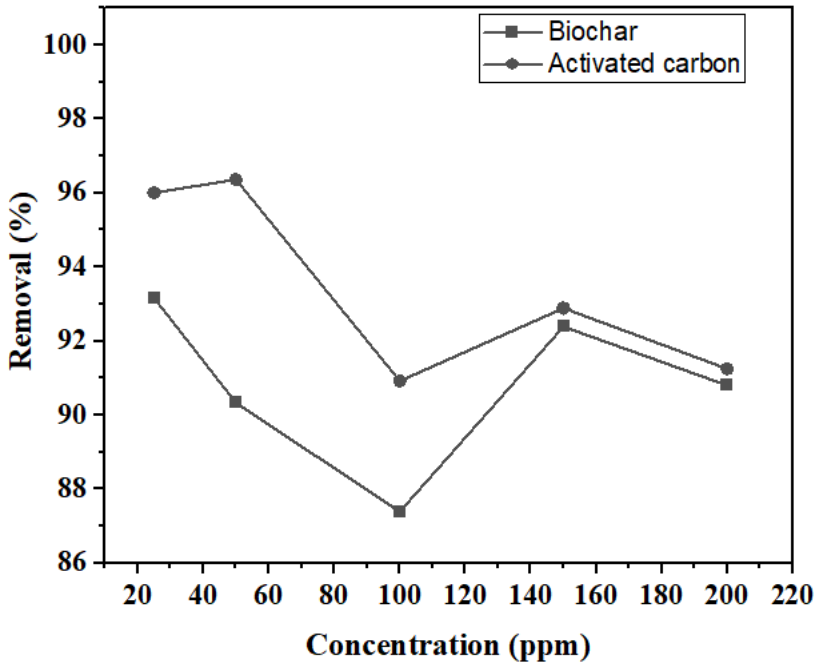

Figure 4.9*: Effect of initial concentration for the removal of Cr(VI)*

4.9 Effect of dosages

The dose of the biosorbent is a crucial factor that affects biosorption. It is possible that an increase in the adsorbent surface region, which increases the number of adsorption sites available for adsorption, is the cause of the initial increase in the percentage of metallic ions adsorbed that is observed with an increase in biosorbent dosages. The concentration gradient between adsorbate and biosorbent may cause a decrease in the percentage of metal ions biosorbed at biosorbent doses above the optimal dosage value. The amount of metallic ions adsorbed per gram of biomass may decrease as biomass concentration is raised. In a few experiments, removal reaches a peak and then declines as a result of the sorbent becoming saturated (Gupta et al., 2020). In the following figure 4.10, effect of dosage of biochar (a) and activated carbon (b) for the removal of Cr(VI)

are plotted. The optimum dosage of biochar and activated carbon are found to be 1 g/L i.e. 50 mg/50 mL Cr(VI) solution.

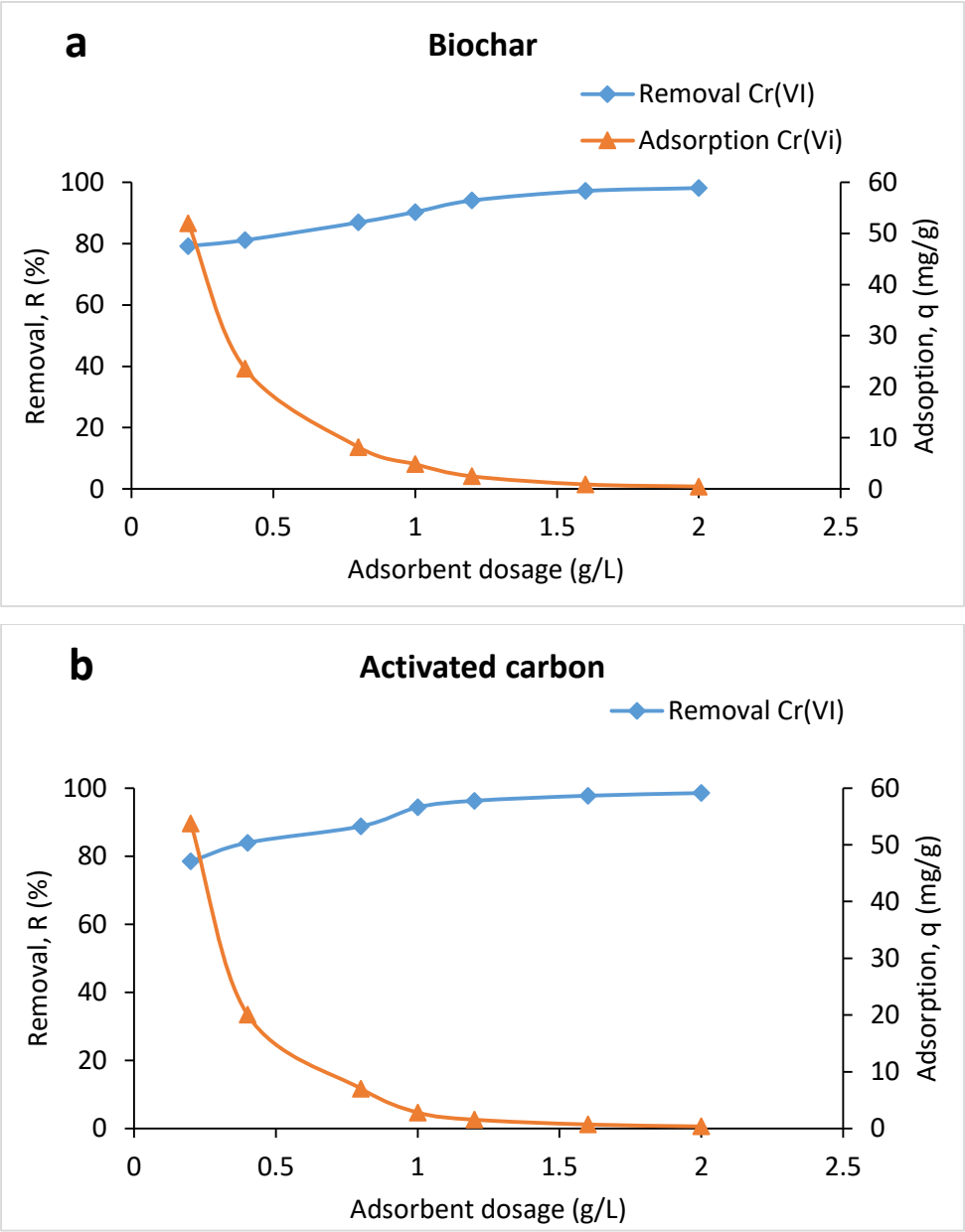

Figure 4.10*: Effect of dosage of carbon for the removal of Cr(VI)*

4.10 Effect of Time

The effect of contact time was examined in order to determine the best time for Cr(VI) sorption on biosorbents. Figure 4.9 indicates the percentage of Cr(VI) removed using

activated carbon and biochar, respectively. The graph shows the average removal capacity of activated carbon and biochar at various contact times. When the contact duration reached two hours, the activated carbon could remove 80.8 % of the Cr(VI) from solution, while biochar could remove 70.92 % of the Cr(VI). In the case of sorption capacity, biochar absorbed 35.46 mg/g average Cr (VI) from solution, whereas activated carbon removed an average of 40.40 mg/g Cr (VI) at 120 min. The Cr(VI) removal efficacy could be explained as follows:

The Cr(VI) ions diffused into the biosorbent's pores and were largely absorbed electrostatically in the porous surface and the amount of sorption active sites got declined accordingly. The remaining ions' diffusion or adsorption becomes saturated as contact time exceeds 120 minutes (figure 4.11). The sorption rate got reduced with longer contact times as a result of competition between Cr(VI) ions and the less abundant surface active sites (Khalil et al., 2020).

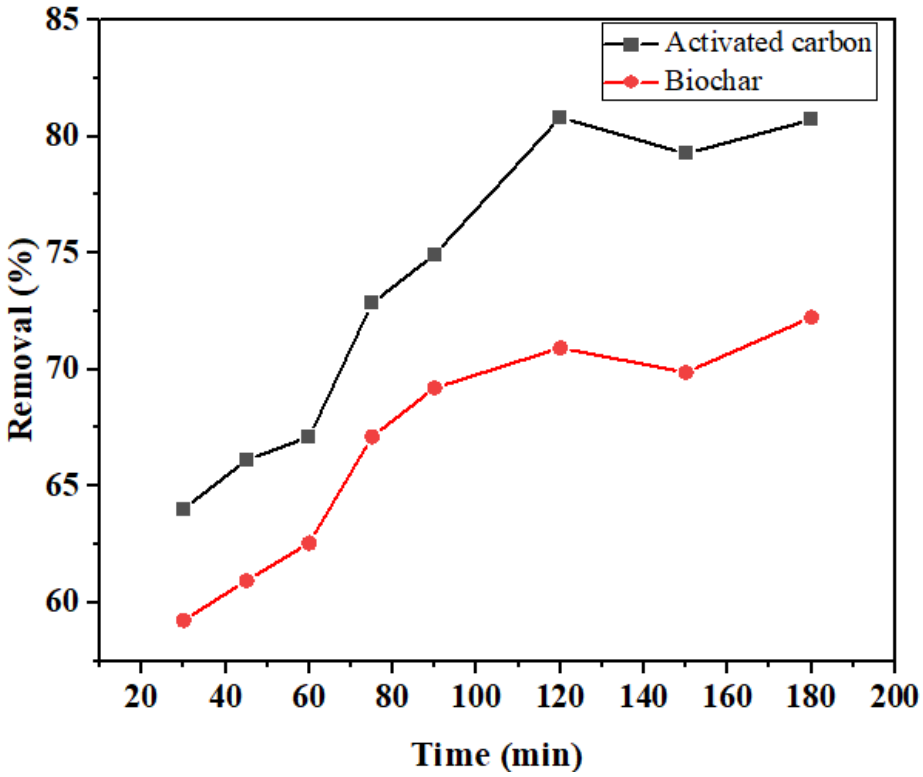

Figure 4.11*: Effect of agitation time for the removal of Cr(VI)*

4.11 Adsorption Isotherm

4.11.1 Freundlich Isotherm

The Freundlich isotherm model takes into consideration the multilayer adsorption of Cr(VI) on the heterogeneous surface of the adsorbents, and it shows that as the

adsorption sites of the adsorbents are fully occupied, the adsorption energy rapidly declines (Rai et al., 2021). The Freundlich isotherm, which was initially created as a model of empirical data, can be expressed as follows.

$$qe = K_f \times Ce^{1/n} \quad \ldots (8)$$

Where, k_f represents Freundlich isotherm and 1/n represents Freundlich exponent. The above equation can be reformulated into following linear equation:

$$\log qe = \frac{1}{n}\log Ce + \log K_f \quad \ldots (9)$$

The above linear form of the equation can be used to determine whether the adsorption process fulfills the Freundlich isotherm and to determine the constants, much like the Langmuir adsorption isotherm (Chung et al., 2015).

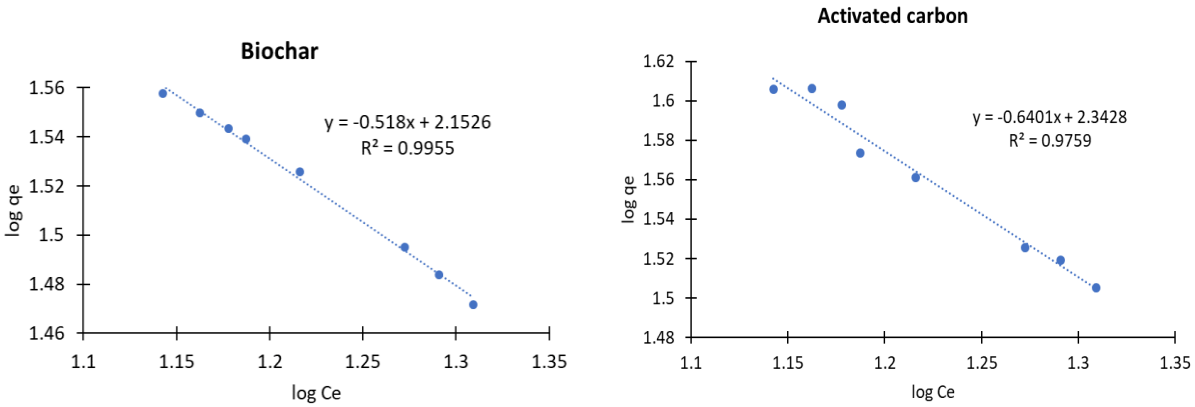

Figure 4.12*: Freundlich adsorption isotherm fitted for biochar and activated carbon*

Table 4.3: *Table showing Freundlich constant and R^2 value*

Adsorbent	Exp.q_{max}	Freundlich Isotherm		
		Slope(1/n)	K_f or b	R^2
Activated carbon	40.401	-0.6401	220.191	0.9759
Biochar	35.462	-0.518	142.21	0.9955

4.11.2 Langmuir Isotherm

The concept behind the Langmuir isotherm is that "maximal adsorption occurs when a saturated monolayer of solute molecules is present on the adsorbate surface." Adsorbate molecules do not migrate in the plane of the surface, and the energy of the adsorbant is constant (Adhikari, D. L., Aryal, R. L., Bhattarai, S., Gautam, S. K., & Poudel, 2017).

Fundamental assumptions behind the Langmuir isotherm include monolayer adsorption, homogeneous distribution of adsorption sites, constant adsorption energy, and minimal interaction between adsorbate molecules (Wang & Guo, 2020). It can be expressed into following linear equation:

$$\frac{Ce}{qe} = \left(\frac{1}{K_L \times qmax}\right) + \frac{Ce}{qmax} \quad \ldots (7)$$

Where, Ce is the solute concentration, or so-called adsorbate, in the solution at equilibrium (in mg/L), qe is the solute mass adsorbed per unit adsorbent mass at equilibrium (in mg/g), K_L is the constant of the Langmuir isotherm (in mg/L), and qmax is the maximum adsorption capacity (in mg/g) (Chung et al., 2015).

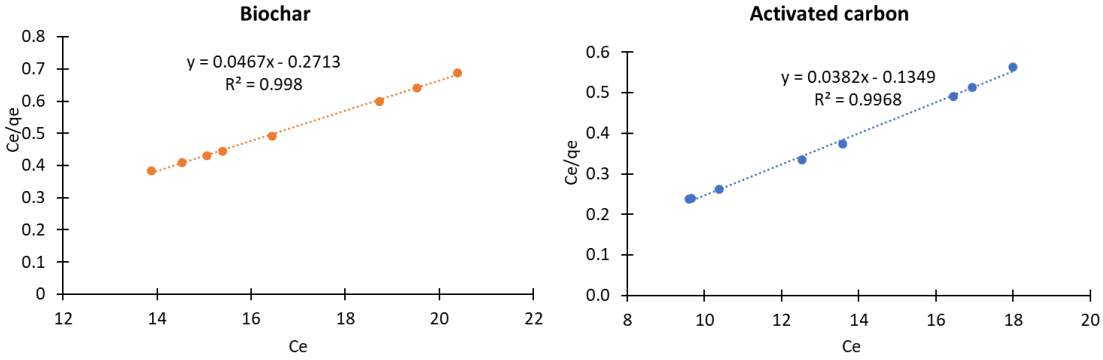

Figure 4.13*: Langmuir adsorption isotherm for activated carbon and biochar*

Table 4.4: *Table showing Langmuir adsorption constant and R^2 value*

Adsorbent	Exp. q_{max}	Langmuir Isotherm		
		qm	K_L or b	R^2
Activated	40.401	26.178	-0.2823	0.9968
Biochar	35.462	21.413	-0.1721	0.998

According to the Langmuir isotherm model, the R^2 values for activated and biochar were found to be 0.99683 and 0.99798, respectively. These values fall in the range of $0 < R_L < 1$, indicating that the process is favorable and the adsorption data are well fit for the Langmuir adsorption isotherm.

4.12 Adsorption Kinetics

To understand the kinetics of the Cr(VI) adsorption onto activated and biochar, pseudo-first order and pseudo-second order models were evaluated. The correlation coefficients R^2 were used to represent how well the experimental data matched the values predicted by the model. The model's ability to accurately predict the kinetics of chromium biosorption is indicated by a relatively high R^2 (values close to or equal to 1). By first converting the kinetic constants into a linear form, which transforms the equation, and then by using a linear regression, it is possible to determine the kinetic constants for the models in the simplest way possible. The most popular technique for fitting a straight line through experimental results is least squares. The goal of least squares is to locate the line between the experimental points and the straight line that maximizes the coefficient of determination, or R^2, between them (Sahmoune & Louhab, 2010).

The linear equation for pseudo-first order model is given by:

$$\log(qe - qt) = \log qe - \frac{k_t}{2.303} t \quad \ldots (10)$$

A plot of log(qe - qt) Vs time (t) for the Cr(VI) is in figure 4.12.

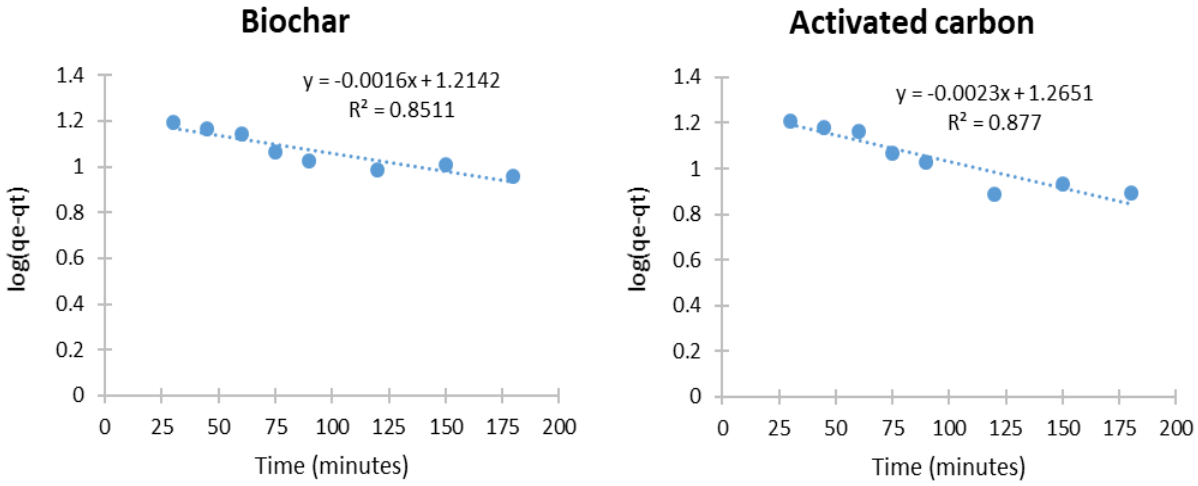

Figure 2.14*: Pseudo first order kinetics for biochar and activated carbon*

The linear equation for the pseudo order model is given by

$$\frac{t}{q_t} = \frac{1}{k_2 qe^2} + \frac{1}{qe} t \quad \ldots (11)$$

A plot t/qt Vs time for the Cr(VI) is in figure 4.15.

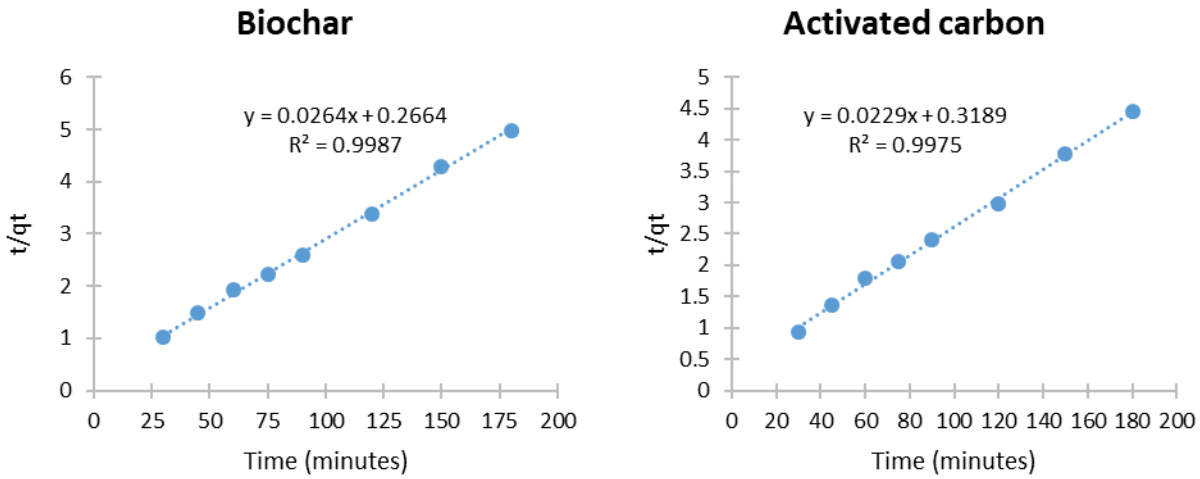

Figure 4.15*: Pseudo second order kinetics for biochar and activated carbon*

The different kinetic parameter for pseudo-first and pseudo-second order kinetics are summarized in table

Table 4.5: *Table showing pseudo first and second order kinetic parameters*

Biomass	Pseudo-First order kinetics			Pseudo-second order kinetics		
	q_e	K_1	R^2	q_e	K_1	R^2
Activated carbon	18.412	0.0053	0.877	43.668	0.00164	0.9975
Biochar	16.376	0.00368	0.8511	37.879	0.00262	0.9987

CHAPTER 5

5. CONCLUSION

The powder form of *Shorea robusta* bark was prepared by cutting and grinding process. Biochar was obtained by treating the powder form of *Shorea robusta* with concentrated sulphuric acid. Chemical activation of as-synthesized biochar was performed by treating with aqueous solution of zinc chloride at different ratio. The biochar:zinc chloride at 1:5 ratio by mass exhibited the optimum iodine number (iodine number of biochar and activated were 125.73 and 1272.54 mg/g, respectively) and methylene blue number (The methylene blue number of biochar and activated were 124.14 and 147.60 mg/g, respectively). The optimized activated carbonized was heated at an optimized temperature of 300 ℃. Physicochemical characterization of as-synthesized activated carbon was carried out in terms of XRD and FTIR analysis. The surface area and porosity of the activated carbon was carried out by methylene blue number method and iodine number method, respectively. The result showed the microporosity of the activated carbon. Upon activation, the pzc value of activated carbon was changed from 4.62 to 6.16. This showed the adsorption of anionic form of Cr(VI) is feasible below pH 6.

At pH–2, starting concentration (50 mg/L) of Cr(VI), and dose, the best adsorption capacity of activated carbon and biochar was achieved at 50 mg. Both activated carbon and biochar were shown to have maximal adsorption capacities of 48.18 and 45.16 mg/g, respectively. The adsorption data were examined using the Langmuir and Freundlich adsorption isotherm models, where Langmuir's is the best fit. It showed the pseudo second order kinetics in Langmuir adsorption isotherm. All in all, result shows that the activated carbon prepared from bark of *Shorea robusta* could serve as a promising carbon material for the removal of heavy metal ions such as Cr(VI).

Future perspective

In this work, activation of carbon materials could not be carried out due to time and resource constraint. Carbonization of carbon under in inert atmosphere can develop highly porous materials with profound surface area. Besides this, this work was devoted in the removal of Cr(VI) only. Other metal ions can also be assayed for their removal from as-synthesized activated carbon.

REFERENCES

Adeeyinwo, C. E., Okorie, & Idowu, G. O. (2013). Basic Calibration of UV/ Visible Spectrophotometer. *International Journal of Science and Technology*, *2*(3), 247–251.

Adhikari, D. L., Aryal, R. L., Bhattarai, S., Gautam, S. K., & Poudel, B. R. (2017). *Removal of chromium (VI) from aqueous solution using chemically-modified sweet lime (Citrus limetta) Peels as Adsorbent. Journal of Nepal Chemical Society, 36,* (pp. 82–95).

Akar, E., Altinişik, A., & Seki, Y. (2013). Using of activated carbon produced from spent tea leaves for the removal of malachite green from aqueous solution. *Ecological Engineering*, *52*, 19–27.

Anastopoulos, I., Robalds, A., Nguyen, H., & Dimitris, T. (2018). Removal of heavy metals by leaves - derived biosorbents. *Environmental Chemistry Letters*, *0123456789*. https://doi.org/10.1007/s10311-018-00829-x

Asimakopoulos, G., Baikousi, M., Kostas, V., Papantoniou, M., Bourlinos, A. B., Zbořil, R., Karakassides, M. A., & Salmas, C. E. (2020). Nanoporous activated carbon derived via pyrolysis process of spent coffee: Structural characterization. Investigation of its use for hexavalent chromium removal. *Applied Sciences*, *10*(24), 8812.

Attia, A., Khedr, S., & Elkholy, S. (2010). Adsorption of chromium ion (VI) by acid activated carbon. *Brazilian Journal of Chemical Engineering*, *27*, 183–193.

Bansal, R. C., & Goyal, M. (2005). *Activated carbon adsorption*. CRC press.

Belcaid, A., Beakou, B., El Hassani, K., Bouhsina, S., & Anouar, A. (2021). Efficient removal of Cr (VI) and Co (II) from aqueous solution by activated carbon from Manihot esculenta Crantz agricultural bio-waste. *Water Science and Technology*, *83*(3), 556–566.

Bonilla-Petriciolet, A., Mendoza-Castillo, D. I., & Reynel-Ávila, H. E. (2017). Adsorption processes for water treatment and purification. *Adsorption Processes for Water Treatment and Purification*, 1–256. https://doi.org/10.1007/978-3-319-58136-1

Budinova, T., Savova, D., B.Tsyntsarski, Ania, C. O., Cabal, B., Parra, J. B., & Petrov, N. (2009). Biomass waste-derived activated carbon for the removal of arsenic

and manganese ions from aqueous solutions. *Applied Surface Science*, *255*(8), 4650–4657. https://doi.org/10.1016/j.apsusc.2008.12.013

Çeçen, F., & Aktas, Ö. (2011). *Activated carbon for water and wastewater treatment: Integration of adsorption and biological treatment*. John Wiley & Sons.

Chand, P., Shil, A. K., Sharma, M., & Pakade, Y. B. (2014). Improved adsorption of cadmium ions from aqueous solution using chemically modified apple pomace: Mechanism, kinetics, and thermodynamics. *International Biodeterioration & Biodegradation*, *90*, 8–16.

Cheenmatchaya, A., & Kungwankunakorn, S. (2014). Preparation of activated carbon derived from rice husk by simple carbonization and chemical activation for using as gasoline adsorbent. *International Journal of Environmental Science and Development*, *5*(2), 171.

Chung, H. K., Kim, W. H., Park, J., Cho, J., Jeong, T. Y., & Park, P. K. (2015). Application of Langmuir and Freundlich isotherms to predict adsorbate removal efficiency or required amount of adsorbent. *Journal of Industrial and Engineering Chemistry*, *28*, 241–246. https://doi.org/10.1016/j.jiec.2015.02.021

Cotruvo, J. A. J. J. A. W. W. A. (2017). *Guidelines for Drinking-water Quality*.

Cruz, G. J. F., Mondal, D., Rimaycuna, J., Soukup, K., Gómez, M. M., Solis, J. L., & Lang, J. (2020). Agrowaste derived biochars impregnated with ZnO for removal of arsenic and lead in water. *Journal of Environmental Chemical Engineering*, *8*(3). https://doi.org/10.1016/j.jece.2020.103800

Dan, Y., Xu, L., Qiang, Z., Dong, H., & Shi, H. (2021). Preparation of green biosorbent using rice hull to preconcentrate, remove and recover heavy metal and other metal elements from water. *Chemosphere*, *262*, 127940. https://doi.org/10.1016/j.chemosphere.2020.127940

Di Natale, F., Lancia, A., Molino, A., & Musmarra, D. (2007). Removal of chromium ions form aqueous solutions by adsorption on activated carbon and char. *Journal of Hazardous Materials*, *145*(3), 381–390.

Duruibe, J. O., Ogwuegbu, M. O. C., & Egwurugwu, J. N. (2007). Heavy metal pollution and human biotoxic effects. *International Journal of Physical Sciences*, *2*(5), 112–118. https://doi.org/10.1016/j.proenv.2011.09.146

Fendorf, S. E. (1995). Surface reactions of chromium in soils and waters. *Geoderma*, *67*(1–2), 55–71. https://doi.org/10.1016/0016-7061(94)00062-F

Ferhan, C., & Ozgur, A. (2011). *Related Titles Ozonation of Water and Waste Water Introduction to Environmental Engineering Rapid Chemical and Biological Techniques for Water Monitoring Functional Nanostructured Materials and Membranes for Water Treatment Risk Analysis of Water Pollutio* (Issue July).

Franguelli, F. P., Tannous, K., & Cione Coppi, C. (2019). Biosorption of hexavalent chromium from aqueous solutions using raw coconut fiber as a natural adsorbent. *Chemical Engineering Communications*, *206*(11), 1437–1450. https://doi.org/10.1080/00986445.2018.1557154

Garg, U. K., Kaur, M. P., Garg, V. K., & Sud, D. (2007). Removal of hexavalent chromium from aqueous solution by agricultural waste biomass. *Journal of Hazardous Materials*, *140*(1–2), 60–68. https://doi.org/10.1016/j.jhazmat.2006.06.056

Gupta, S., Sireesha, S., Sreedhar, I., Patel, C. M., & Anitha, K. L. (2020). Latest trends in heavy metal removal from wastewater by biochar based sorbents. *Journal of Water Process Engineering*, *38*(May), 101561. https://doi.org/10.1016/j.jwpe.2020.101561

Hafshejani, L. D., Nasab, S. B., Gholami, R. M., Moradzadeh, M., Izadpanah, Z., Hafshejani, S. B., & Bhatnagar, A. (2015). Removal of zinc and lead from aqueous solution by nanostructured cedar leaf ash as biosorbent. *Journal of Molecular Liquids*, *211*, 448–456. https://doi.org/10.1016/j.molliq.2015.07.044

Itodo, a U., Abdulrahman, F. W., Hassan, L. G., Maigandi, S. a, & Itodo, H. U. (2010). Application of Methylene Blue and Iodine Adsorption in the Measurement of Specific Surface Area by four Acid and Salt Treated Activated Carbons . *New York Science Journal*, *3*(5), 25–33.

Katheresan, V., Kansedo, J., & Lau, S. Y. (2018). Efficiency of various recent wastewater dye removal methods: A review. *Journal of Environmental Chemical Engineering*, *6*(4), 4676–4697.

Khalil, U., Bilal Shakoor, M., Ali, S., Rizwan, M., Nasser Alyemeni, M., & Wijaya, L. (2020). Adsorption-reduction performance of tea waste and rice husk biochars for Cr(VI) elimination from wastewater. *Journal of Saudi Chemical Society*, *24*(11), 799–810. https://doi.org/10.1016/j.jscs.2020.07.001

Kumari, D., Goswami, R., Kumar, M., Kataki, R., & Shim, J. (2018). Removal of Cr (VI) ions from the aqueous solution through nanoscale zero-valent iron (nZVI)

Magnetite Corn Cob Silica (MCCS): A bio-waste based water purification perspective. *Groundwater for Sustainable Development, 7*, 470–476.

Lua, A. C., Lau, F. Y., & Guo, J. (2006). Influence of pyrolysis conditions on pore development of oil-palm-shell activated carbons. *Journal of Analytical and Applied Pyrolysis, 76*(1–2), 96–102.

Moosavi, S., Manta, O., El-Badry, Y. A., Hussein, E. E., El-Bahy, Z. M., Mohd Fawzi, N. fariza B., Urbonavičius, J., & Moosavi, S. M. H. (2021). A study on machine learning methods' application for dye adsorption prediction onto agricultural waste activated carbon. *Nanomaterials, 11*(10), 2734.

Mopoung, S. (2008). Surface image of charcoal and activated charcoal from banana peel. *Journal of Microscopy Society of Thailand, 22*, 15–19.

Moussavi, G., & Barikbin, B. (2010). Biosorption of chromium(VI) from industrial wastewater onto pistachio hull waste biomass. *Chemical Engineering Journal, 162*(3), 893–900. https://doi.org/10.1016/j.cej.2010.06.032

Namane, A., Mekarzia, A., Benrachedi, K., Belhaneche-Bensemra, N., & Hellal, A. (2005). Determination of the adsorption capacity of activated carbon made from coffee grounds by chemical activation with ZnCl2 and H3PO4. *Journal of Hazardous Materials, 119*(1–3), 189–194.

Noor, N. M., Othman, R., Mubarak, N. M., & Abdullah, E. C. (2017). Agricultural biomass-derived magnetic adsorbents: Preparation and application for heavy metals removal. *Journal of the Taiwan Institute of Chemical Engineers, 78*, 168–177. https://doi.org/10.1016/j.jtice.2017.05.023

Pandey, P. K., Choubey, S., Verma, Y., Pandey, M., & Chandrashekhar, K. (2009). Biosorptive removal of arsenic from drinking water. *Bioresource Technology, 100*(2), 634–637. https://doi.org/10.1016/j.biortech.2008.07.063

Parlayici, Ş., & Pehlivan, E. (2019). Comparative study of Cr (VI) removal by bio-waste adsorbents: Equilibrium, kinetics, and thermodynamic. *Journal of Analytical Science and Technology, 10*(1), 1–8.

Patil, P., Sawant, D., & Deshmukh, R. (2012). Physico-chemical parameters for testing of water-a review. *International Journal of Environmental Sciences, 3*(3), 1194.

Peng, H., & Guo, J. (2020). Removal of chromium from wastewater by membrane filtration, chemical precipitation, ion exchange, adsorption electrocoagulation, electrochemical reduction, electrodialysis, electrodeionization, photocatalysis

and nanotechnology: A review. *Environmental Chemistry Letters*, *18*(6), 2055–2068.

Prahas, D., Kartika, Y., Indraswati, N., & Ismadji, S. (2008). Activated carbon from jackfruit peel waste by H3PO4 chemical activation: Pore structure and surface chemistry characterization. *Chemical Engineering Journal*, *140*(1–3), 32–42.

Purcell, P. J. (2005). Milestones in the development of municipal water treatment science and technology in the 19th and early 20th centuries: Part I. *Water and Environment Journal*, *19*(3), 230–237.

Qin, L., He, L., Yang, W., & Lin, A. (2020). Preparation of a novel iron-based biochar composite for removal of hexavalent chromium in water. *Environmental Science and Pollution Research*, *27*(9), 9214–9226. https://doi.org/10.1007/s11356-019-06954-6

Rai, R., Karki, D. R., Bhattarai, K. P., Pahari, B., Shrestha, N., Adhikari, S., Gautam, K., Poudel, B. R., & Campus, T. M. (2021). *Recent Advances in Biomass-Based Waste Materials for the Removal of Chromium (VI) from Wastewater: A Review*. *2*(1), 37–50.

Reddy, P. M. K., Verma, P., & Subrahmanyam, C. (2016). Bio-waste derived adsorbent material for methylene blue adsorption. *Journal of the Taiwan Institute of Chemical Engineers*, *58*, 500–508.

Rengaraj, S., Yeon, K.-H., & Moon, S.-H. (2001). Removal of chromium from water and wastewater by ion exchange resins. *Journal of Hazardous Materials*, *87*(1–3), 273–287.

Rocha, C. G., Zaia, D. A. M., Alfaya, R. V. da S., & Alfaya, A. A. da S. (2009). Use of rice straw as biosorbent for removal of Cu(II), Zn(II), Cd(II) and Hg(II) ions in industrial effluents. *Journal of Hazardous Materials*, *166*(1), 383–388. https://doi.org/10.1016/j.jhazmat.2008.11.074

Sahmoune, M. N., & Louhab, K. (2010). Kinetic analysis of trivalent chromium biosorption by dead streptomyces rimosus biomass. *Arabian Journal for Science and Engineering*, *35*(2 A), 69–80.

Şen, A., Pereira, H., Olivella, M. A., & Villaescusa, I. (2015). Heavy metals removal in aqueous environments using bark as a biosorbent. *International Journal of Environmental Science and Technology*, *12*(1), 391–404. https://doi.org/10.1007/s13762-014-0525-z

Shakoor, M. B., Niazi, N. K., Bibi, I., Murtaza, G., Kunhikrishnan, A., Seshadri, B., Shahid, M., Ali, S., Bolan, N. S., Ok, Y. S., Abid, M., & Ali, F. (2016). Remediation of arsenic-contaminated water using agricultural wastes as biosorbents. *Critical Reviews in Environmental Science and Technology*, *46*(5), 467–499. https://doi.org/10.1080/10643389.2015.1109910

Shrestha, D., Maensiri, S., Wongpratat, U., Lee, S. W., & Nyachhyon, A. R. (2019). Shorea robusta derived activated carbon decorated with manganese dioxide hybrid composite for improved capacitive behaviors. *Journal of Environmental Chemical Engineering*, *7*(5), 103227. https://doi.org/10.1016/j.jece.2019.103227

Tan, I., Ahmad, A., & Hameed, B. (2008). Adsorption of basic dye on high-surface-area activated carbon prepared from coconut husk: Equilibrium, kinetic and thermodynamic studies. *Journal of Hazardous Materials*, *154*(1–3), 337–346.

Verma, A., Dhanik, J., Belal, B., & Prakash, O. (2017). *Bio sorption of heavy metal Chromium (III) from synthetic waste water using Taxus baccata bark as bio adsorbent*. *5*(4), 1758–1761.

Wang, J., & Guo, X. (2020). Adsorption isotherm models: Classification, physical meaning, application and solving method. *Chemosphere*, *258*, 127279. https://doi.org/10.1016/j.chemosphere.2020.127279

Wu, F.-C., Tseng, R.-L., & Juang, R.-S. (1999). Pore structure and adsorption performance of the activated carbons prepared from plum kernels. *Journal of Hazardous Materials*, *69*(3), 287–302.

Yang, J., & Qiu, K. (2010). Preparation of activated carbons from walnut shells via vacuum chemical activation and their application for methylene blue removal. *Chemical Engineering Journal*, *165*(1), 209–217. https://doi.org/10.1016/j.cej.2010.09.019

Zhang, H., Yan, Y., & Yang, L. (2010). Preparation of activated carbon from sawdust by zinc chloride activation. *Adsorption*, *16*(3), 161–166.